Mathematical Models and Methods in Applied Sciences

AGGREGATION VIA THE NEWTONIAN POTENTIAL AND AGGREGATION PATCHES

ANDREA L. BERTOZZI
University of California Los Angeles, Department of Mathematics
Los Angeles, CA 90095, USA
bertozzi@math.ucla.edu

THOMAS LAURENT
University of California Riverside, Department of Mathematics
Riverside, CA 92521, USA
laurent@math.ucr.edu

FLAVIEN LÉGER*
University of California Los Angeles, Department of Mathematics
Los Angeles, CA 90095, USA
flavien@math.ucla.edu

Received (Day Month Year)
Revised (Day Month Year)
Communicated by (xxxxxxxxxx)

This paper considers the multidimensional active scalar problem of motion of a function $\rho(x,t)$ by a velocity field obtained by $v = -\nabla N * \rho$, where N is the Newtonian potential. We prove well-posedness of compactly supported $L^\infty \cap L^1$ solutions of possibly mixed sign. These solutions include an important class of solutions that are proportional to characteristic functions on a time-evolving domain. We call these *aggregation patches*. Whereas positive solutions collapse on themselves in finite time, negative solutions spread and converge toward a self-similar spreading circular patch solution as $t \to \infty$. We give a convergence rate that we prove is sharp in 2D. In the case of positive collapsing solutions, we investigate numerically the geometry of patch solutions in 2D and in 3D (axisymmetric). We show that the time evolving domain on which the patch is supported typically collapses on a complex skeleton of codimension one.

Keywords: active scalar; nonlocal transport; aggregation; Newtonian potential.

AMS Subject Classification: 35Q35, 35Q70, 35Q92, 31B10, 34G25, 76B03

*current address: CMLA, ENS Cachan, 61 avenue du Président Wilson 94235 Cachan Cedex

1. Introduction

Consider the aggregation equation

$$\frac{\partial \rho}{\partial t} + \mathrm{div}(\rho v) = 0, \quad v = -\nabla N * \rho \tag{1.1}$$

where N is the Newtonian potential in $\mathbb{R}^d$ for $d \geq 2$. For more general interaction kernels K, this problem has been a very active area of research in the literature [5,9,10,7,12,14,15,16,17,18,19,20,21,24,27,29,35,30,36,38,42,43,44,46,45,53,54,62,63,64]. These models arise in a number of applications including aggregation in materials science [36,56,57], cooperative control [35], granular flow [25,26,64], biological swarming models [53,52,62,63], evolution of vortex densities in superconductors [34,2,1,33,51] and bacterial chemotaxis [19,38,15,16]. A body of recent work has focused on the problem of finite time singularities and local vs global well-posedness in multiple space dimensions for both the inviscid case (1.1) [9,10,11,7,12,17,13,24,30,37,42] and the cases with various kinds of diffusion [4,15,13,43,44]. The highly studied Keller-Segel problem typically has a Newtonian potential and linear diffusion. For the pure transport problem (1.1), of particular interest is the transition from smooth solutions to weak and measure solutions with mass concentration.

In two space dimensions, equation (1.1) with the Newtonian potential arises as a model for the evolution of vortex densities in superconductors [34,60,59,47,2,1,48,49,33,51], and also in models for adhesion dynamics[56,57]. These problems are known to develop finite time singularities and several papers have considered the existence of solutions with measure initial data [33,57,1]. Among others, our manuscript develops a complete theory of weak solution in arbitrary dimension for the case where the density function ρ is bounded, compactly supported and has mixed sign. Our theory includes sharp well-posedness for L^∞ data including the maximal time interval of existence.

1.1. *Description of the problem and well-posedness theory*

Here we use the convention that $\Delta N = \delta$, with this convention the interaction kernel is attractive for positive ρ. Using the fact that $\mathrm{div} v = -\Delta N * \rho = -\rho$, equation (1.1) can be rewritten

$$\frac{\partial \rho}{\partial t} + \nabla \rho \cdot v = \rho^2, \quad v = -\nabla N * \rho \tag{1.2}$$

and therefore the values of ρ satisfies the ODE $\dot{y} = y^2$ along the "characteristics" defined by

$$\frac{d}{dt} X^t(\alpha) = v(X^t(\alpha), t), \quad X^0(\alpha) = 0. \tag{1.3}$$

Solving $\dot{y} = y^2$ gives the formulas

$$\rho(X^t(\alpha), t) = \left(\frac{1}{\rho_0(\alpha)} - t \right)^{-1} \quad \text{and} \quad \rho(x,t) = \left(\frac{1}{\rho_0(X^{-t}(x))} - t \right)^{-1} \tag{1.4}$$

where $X^{-t} : \mathbb{R}^d \to \mathbb{R}^d$ is the inverse of the mapping X^t. It is clear from (1.4) that if ρ_0 is strictly positive somewhere, then the first blow-up occurs at time

$$t = \frac{1}{\sup_{x\in\mathbb{R}^d} \rho_0(x)}.$$

On the other hands if $\rho_0(x) \leq 0$ for all x, the values on every characteristic converge to zero as $t \to +\infty$ and no blowup occurs. These argument will be made rigorous in Section 2, where we prove existence and uniqueness of compactly supported bounded solutions of mixed sign on the time interval $[0, T]$ with

$$T < (\sup \rho_0)^{-1}.$$

If the initial data is negative, then $(\sup \rho_0)^{-1} = +\infty$ and therefore solutions exists for all $t > 0$. The theory is first carried out in Lagrangian variables for functions ρ that are Hölder continuous, using the classical Picard theory on a Banach space, thus proving both existence and uniqueness. Then we prove existence for L^∞ functions by passing to the limit in smooth approximations, also using Lagrangian variables for the passage to the limit. However the resulting solution is a classical solution in the sense of distributions, in Eulerian variables. Uniqueness of L^∞ solutions is proved using well-known H^{-1} energy estimates for the Eulerian form of the problem, we do not include the proof but rather refer the reader to the extensive literature using these techniques, dating back to the seminal paper of Yudovich[65] for L^∞ vorticity for the 2D Euler problem.

1.2. *Aggregation patches*

We now discuss aggregation patches, solutions of (1.1) with initial data

$$\rho_0(x) = c\, \chi_{\Omega_0}(x)$$

where c is a (possibly negative) constant and $\chi_{\Omega_0}(x)$ is the characteristic function of the bounded domain $\Omega_0 \subset \mathbb{R}^d$. Note that such initial data are compactly supported and belong to $L^1 \cap L^\infty$ therefore the well-posedness theory from the section 2 applies. These solutions are analogues of the famous *vortex patch* solutions of the 2D incompressible Euler equations [6,28,22,32,31,66]. However for the aggregation problem, the patch solutions exist in any dimension. From (1.4) we see that

$$\rho(x,t) = \left(\frac{1}{c} - t\right)^{-1} \chi_{\Omega_t}(x). \tag{1.5}$$

where $\Omega_t = X^t(\Omega_0)$ is a time evolving domain and the mapping $X^t : \mathbb{R}^d \to \mathbb{R}^d$ is defined by (1.3). Because mass is conserved we necessarily have

$$|\Omega_t| = (1 - ct)\, |\Omega_0|$$

where $|\Omega_t|$ stands for the Lebesgue measure of Ω_t. Therefore positive patches (i.e. $c > 0$) collapse to a domain of Lebesgue measure 0 at time $t = 1/c$. In contrast,

the Lebesgue measure of negative patches (i.e. $c < 0$) is increasing linearly in time. The simplest patch solutions are the circular patches

$$\rho(x,t) = \left(\frac{1}{c} - t\right)^{-1} \chi_{\Omega_t}(x), \quad \Omega_t = B(0, R(t)), \quad R(t) = R_0 \left(1 - ct\right)^{1/d}. \quad (1.6)$$

They are explicit self-similar solutions to (1.1). In section 3 we show that in the case of negative L^∞ spreading solutions, these self-similar circular patches are global attractor of the dynamics. Moreover we prove that the convergence rate toward these global attractors is given by

$$\|\rho(\cdot,t) - \Phi(\cdot,t)\|_{L^1} \leq Ct^{-\lambda}, \qquad \lambda = \frac{1}{2^{d-1}}$$

where $\rho(x,t)$ is a negative solution and $\Phi(x,t)$ is a spreading negative circular patch. Note in particular that this give a convergence rate in $1/\sqrt{t}$ in two dimensions.

In section 4 we give an explicit formula for an elliptical patch in two dimensions. In the collapsing case, the finite time singularity results in convergence to a weighted measure along an interval of length $2(a_0 - b_0)$ where a_0 is the length of the semi-major axis of the initial data and b_0 is the length of the semi-minor axis (Theorem 4.1). We then show that the L^1 difference between an elliptic spreading patch and a circular one decays like $1/\sqrt{t}$ (Theorem 4.2), therefore proving the sharpness of our convergence rate in 2D. The remainder of section 4 is devoted to a numerical study of the different patch evolutions in 2D and 3D for both the spreading and collapsing problem. The 3D solutions shown are axisymmetric which allows for a reduction of the computational complexity to that of the 2D problem. In both cases we reduce the numerical simulation to a self-deforming curve in the plane by using a contour dynamics formalism, similar to what has been done for vortex patches in 2D.

Whereas an elliptical patch collapses toward a singular measure supported on a line segment, more general 2D aggregation patches are observed numerically to converge toward singular measures supported on more complex domains, also of codimension one, often consisting of the union of several curves. We refer to this union of intersecting curves as the skeleton of the patch at the collapse time. However this shape is not the topological skeleton of the initial data. In 3D, aggregation patches typically converge toward singular measure uniformly distributed on the union of intersecting surfaces, see Figure 6.

In the spreading case we numerically observe a "pinching" phenomena in which the solution clearly converges in L^1 to the circular patch solution as predicted by the analysis, however the boundary does not necessarily converge to a circle. For some initial data the boundary "pinches", creating defects which consist of slits cutting into the circular shape, see Figure 3. These defects may not disappear in the long run. For 3D toroidal initial data the spreading problem deforms to fill a sphere in 3D, while preserving the toroidal topology of the initial data. In this case there is a natural slit that forms related to the preserved topology of the torus.

1.3. *Relationship with the existing literature*

In an earlier paper, two of the authors[11] have shown that the problem considered here reduces to the inviscid Burgers equation for the case of radially symmetric data in any space dimension. This observation has been made for the one dimensional problem in earlier papers, but not for multiple dimensions. The connection to Burgers equation allows us to understand many features of this problem via exact solutions with radial symmetry. The general theory of the equations, considered here, has roots in many previous papers in the literature. Section 2 is largely inspired by chapters four and eight of the book on *Vorticity and Incompressible Flow*[50] however some of these ideas and other ideas have been used to study this aggregation problem in prior papers. Lin and Zhang[47] have studied our problem for spreading case (corresponding to negative sign initial data in our model) in two dimensions and develop general existence theory for data a measure of a fixed sign. Their techniques are similar to the ones we use for existence of L^∞ solutions of mixed sign and come from well-known methods in incompressible fluid dynamics. Our work generalizes their existence results to the mixed sign problem in general dimension and also considers asymptotic behavior of the spreading problem in general dimension. Nieto, Poupaud, and Soler[56] consider our problem in general dimension for data that is in $W^{1,\infty}(\mathbb{R}^d)$ - these results being most relevant to our existence theory for Hölder continuous solutions. They also consider L^∞ data for the spreading problem in general dimension and for the collapsing problem in one space dimension - corresponding to the case of Lipschitz solutions of the inviscid Burgers equation. For the spreading problem they use methods involving entropies and energy estimates in Eulerian variables - these methods are best applied to the spreading problem. Our results for L^∞ data involve solutions with mixed sign, and the existence theory is done mainly in Lagrangian variables using uniform estimates for the particle paths. Masmoudi and Zhang[51] consider a closely related problem, where the sign of the density changes the sign of the velocity field. They establish well-posedness theory in $W^{1,p}$, $p > 2$, and in C^γ for $0 < \gamma < 1$. Mainini[49] considers our problem in L^∞ but without collapse and uses optimal transport theory. Another very related problem is the Chapman-Rubinstein-Schatzman model[2,1] which involves an interaction kernel that is the fundamental solution of $(I - \Delta)$ on a bounded domain with Dirichlet boundary condition. That literature makes heavy use of optimal transport theory.

Regarding the global attractor for the spreading problem, Caffarelli and Vazquez[23] recently consider the dynamics of fractional diffusion, which can be written in our formulation, only with more singular potentials corresponding to $(-\Delta)^{-s}$ where $0 < s < 1$ (our problem corresponds to the case $s = 1$). Note that the corresponding kernel operators are of the form $|x|^{-p}$ where $p = d - 2s$. For these more singular kernels there is a gain of regularity in the solution as the problem is diffusive going forward in time. It has some properties similar to the porous media equation. They prove convergence to the global attractor for these more singular kernels using entropy methods. Compared to this work, we prove convergence to

the global attractor via a direct estimate on the size of the support of the solution and we obtain a convergence rate in L^1.

Models of vortex patches date back to the classical example of the Kirchoff ellipse[40] which has been extensively studied in straining flows[8,55,39]. Numerical simulations of the general vortex patch problem date back to work of Zabusky, Huges, and Roberts [66] and resulted in speculation about the global regularity of the vortex patch boundary [22,32] which was finally settled analytically by Chemin[28] and reproved using potential theory estimates by Bertozzi and Constantin[6]. To the best of our knowledge, the numerical simulation of the aggregation problem and the observation that aggregation patches collapse to complex skeletons of codimension one are new.

2. General well-posedness theory for compactly supported L^∞ solutions of mixed sign

To avoid complications at infinity, for which we know of no physically interesting cases, we simplify the problem by considering compactly supported data, so that the data is also automatically in L^1 due to the essential supremum bound.

2.1. *Well-posedness theory for Hölder continuous densities* $C_0^\gamma(\mathbb{R}^d)$

In this section we derive the well-posedness theory for densities $\rho \in C_0^\gamma(\mathbb{R}^d)$, functions that are Hölder continuous, and that have compact support. We note that the problem is studied in [56] for the case of $W^{1,\infty}$ densities, which would suffice for our purposes here. However for completeness we present an argument in Hölder spaces and will use this, including the compact support, to prove well-posedness of general L^∞ solutions and also to prove a result on long time behavior, which require estimates on the support of the solution. The proof uses ODEs on Banach spaces in Lagrangian coordinates. The ODE (1.3) defining the particle path $t \mapsto X^t(\alpha)$ can be written

$$\frac{d}{dt}X^t(\alpha) = -\int_{\mathbb{R}^d} \nabla N(X^t(\alpha) - y)\rho(y,t)dy.$$

The change of variables $y = X^t(\alpha')$ gives

$$\frac{d}{dt}X^t(\alpha) = -\int_{\mathbb{R}^d} \nabla N(X^t(\alpha) - X^t(\alpha'))\rho(X^t(\alpha'),t)\det(\nabla_\alpha X^t(\alpha'))d\alpha'.$$

However note that if we define $Q(\alpha,t) = \det(\nabla_\alpha X^t(\alpha))$ then Q satisfies

$$\frac{d}{dt}Q(\alpha,t) = \mathrm{div}v(X^t(\alpha),t)\ Q(\alpha,t) = -\rho(X^t(\alpha),t)\ Q(\alpha,t).$$

But since $\frac{d}{dt}\rho(X^t(\alpha),t) = \rho(X^t(\alpha),t)^2$ we see that $\rho(X^t(\alpha),t)Q(\alpha,t)$ is constant in time. Using the fact that $Q(\alpha,0) = 1$ we obtain the following Lagrangian formula-

tion of (1.1):

$$\frac{d}{dt}X^t(\alpha) = -\int_{\mathbb{R}^d} \nabla N(X^t(\alpha) - X^t(\alpha'))\rho(\alpha', 0)Q(\alpha', 0)d\alpha'$$
$$= -\int_{\mathbb{R}^d} \nabla N(X^t(\alpha) - X^t(\alpha'))\rho_0(\alpha')d\alpha'. \tag{2.1}$$

We then define the Banach space on which to work:

$$B = \{X : \mathbb{R}^d \to \mathbb{R}^d \quad \text{such that} \quad \|X\|_{1,\gamma} < \infty\}, \tag{2.2}$$
$$\|X\|_{1,\gamma} = |X(0)| + \|\nabla_\alpha X\|_{L^\infty} + |\nabla_\alpha X|_\gamma, \tag{2.3}$$

where $|\cdot|_\gamma$ stands for the standard Hölder semi-norm. We write our problem as

$$\frac{d}{dt}X^t = F(X^t), \qquad X^0 = \mathrm{Id} \tag{2.4}$$

where $F : B \to B$ is defined by

$$F(X)(\alpha) = -\int_{\mathbb{R}^d} \nabla N(X(\alpha) - X(\alpha'))\ \rho_0(\alpha')d\alpha'. \tag{2.5}$$

Theorem 2.1. *(Local existence and continuation of $C^{1,\gamma}$ particle paths) Consider an initial density ρ_0 that is Hölder continuous and with compact support. Then the initial value problem* (2.4)–(2.5) *has a unique solution on a maximal time interval of existence $[0, T^*)$. Either T^* is infinite or the Banach norm (2.3) blows up as $t \to T^*$.*

Remark 2.1. Although we prove well-posedness of the problem in the Lagrangian formulation, this result implies existence of a solution to the problem in original Eulerian variables (1.1). This is discussed in detail for the Euler problem in Chapter 4 of [50] and is proved rigorously for the weaker case of L^∞ data in the next subsection.

Proof. The proof is similar to the local existence proof of the vorticity formulation of Euler equation in Chapter 4 of [50] and therefore here we just discuss a few key points. In order to apply the Picard theorem on a Banach space, the hardest part is to show that $F : B \to B$ is Lipschitz. We focus on the calculation of the first variation with respect to X. That results in a linear operator which we write as

$$\frac{\delta F}{\delta X}Y := \frac{d}{d\epsilon}F(X + \epsilon Y)|_{\epsilon=0}$$
$$= -\frac{d}{d\epsilon}\int \nabla N(X(\alpha) - X(\alpha') + \epsilon[Y(\alpha) - Y(\alpha')])\rho_0(\alpha')d\alpha'|_{\epsilon=0}$$
$$= -\int D^2 N(X(\alpha) - X(\alpha'))[Y(\alpha) - Y(\alpha')]\rho_0(\alpha')d\alpha'.$$

Following the arguments in chapter four of [50] (see for example Proposition 4.2) we obtain

$$||\frac{\delta F}{\delta X}Y||_{1,\gamma} \leq C(||X||_{1,\gamma})||\rho_0||_\gamma||Y||_{1,\gamma}, \tag{2.6}$$

where $||X||_\gamma = \|X\|_{L^\infty} + |X|_\gamma$. This show the Lipshitz continuity of F. We refer the reader to Chapter 4 of [50] for the details of this calculation. □

Define $|\cdot|_{max}$ and $|\cdot|_{min}$ as follow:

$$|f|_{max} = \sup_{x\in\mathbb{R}^d} f(x) \quad \text{and} \quad |f|_{min} = -\inf_{x\in\mathbb{R}^d} f(x). \tag{2.7}$$

Let us emphasis that $|f|_{min} \geq 0$. Also we obviously have

$$\frac{1}{2}(|f|_{min} + |f|_{max}) \leq \|f\|_{L^\infty} \leq |f|_{min} + |f|_{max}\,. \tag{2.8}$$

Theorem 2.2. $T^* = 1/\left|\rho_0\right|_{max}$.

Note that if $\rho_0 \leq 0$ and compactly suported then $|\rho_0|_{max} = 0$ and $T^* = +\infty$. The rest of this subsection is devoted to the proof of Theorem 2.2. We follow arguments similar to the classical Beale-Kato-Majda theorem for the 3D Euler equation [3], in particular the alternate Hölder space proof from Chapter 4 of [50].

Suppose that the classical solution $\rho(x,t)$ given by Theorem (2.1) exists on a time interval $[0,T)$. Since it is a classical solution it satisfies (1.4) along the particle path. We therefore see that T can not be strictly greater than $1/\left|\rho_0\right|_{max}$, otherwise the solution would blow up and leave the space of continuous functions. This implies that $T^* \leq 1/\left|\rho_0\right|_{max}$. We then now show that if the time interval $[0,T)$ on which the solution is defined is such that $T < 1/\left|\rho_0\right|_{max}$, then there exists a constant C such that

$$\|X^t\|_{1,\gamma} < C \qquad \text{for all } t \in [0,T), \tag{2.9}$$

therefore giving $T^* \geq 1/\left|\rho_0\right|_{max}$ and concluding the proof.

We now prove (2.9) under the condition $T < 1/\left|\rho_0\right|_{max}$. Define the constant

$$k = 1 - T|\rho_0|_{max} \quad \text{and} \quad K = 1 + T|\rho_0|_{min}. \tag{2.10}$$

Clearly $0 < k \leq 1$ and $K \geq 1$. Note that because of (1.4) we have the uniform bounds

$$|\rho_0|_{max} \leq |\rho(\cdot,t)|_{max} = \left(\frac{1}{|\rho_0|_{max}} - t\right)^{-1} \leq \frac{|\rho_0|_{max}}{k} \tag{2.11}$$

$$\frac{|\rho_0|_{min}}{K} \leq |\rho(\cdot,t)|_{min} = \left(\frac{1}{|\rho_0|_{min}} + t\right)^{-1} \leq |\rho_0|_{min} \tag{2.12}$$

for all $t \in [0,T]$. Therefore, from (2.8),

$$\frac{\|\rho_0\|_{L^\infty}}{2K} \leq \frac{|\rho_0|_{min} + |\rho_0|_{max}}{2K} \leq \|\rho(\cdot,t)\|_{L^\infty} \leq \frac{|\rho_0|_{min} + |\rho_0|_{max}}{k} \leq \frac{2\|\rho_0\|_{L^\infty}}{k} \tag{2.13}$$

for all $t \in [0,T]$. We then prove the following elementary estimate:

Lemma 2.1. *For all* $t \in [0, T)$

$$|\rho(\cdot, t)|_\gamma \leq \frac{|\rho_0|_\gamma}{k^2} \left\|\nabla_x X^{-t}\right\|_{L^\infty}^\gamma . \tag{2.14}$$

Proof. From (1.4), we have:

$$\rho(x, t) = \frac{\rho_0(X^{-t}(x))}{1 - \rho_0(X^{-t}(x))t}. \tag{2.15}$$

Then we write:

$$\begin{aligned} |\rho(x,t) - \rho(y,t)| &= \left| \frac{\rho_0(X^{-t}(x)) - \rho_0(X^{-t}(y))}{(1 - \rho_0(X^{-t}(x))t)(1 - \rho_0(X^{-t}(y))t)} \right| \\ &\leq \frac{1}{k^2} \left|\rho_0(X^{-t}(x)) - \rho_0(X^{-t}(y))\right| \\ &\leq \frac{1}{k^2} |\rho_0|_\gamma \left\|\nabla_x X^{-t}\right\|_{L^\infty}^\gamma |x - y|^\gamma . \end{aligned}$$

□

We need then need the following potential theory lemma from [50] (Lemmas 4.5 and 4.6 on page 144):

Lemma 2.2. *Consider* $f \in C^\gamma(\mathbb{R}^d; \mathbb{R}^d)$, $0 < \gamma < 1$, *be a compactly supported function with supported in the ball of radius* R. *Then there exists a constant* C *independent of* R *and* f *such that*

$$\|PVN_{ij} * f\|_{L^\infty} \leq C\{|f|_\gamma \epsilon^\gamma + \max(1, \ln \frac{R}{\epsilon})\|f\|_{L^\infty}\}, \quad \forall \epsilon > 0, \tag{2.16}$$

$$|PVN_{ij} * f|_\gamma \leq C|f|_\gamma. \tag{2.17}$$

Here $PVN_{ij} * f$ *denotes the principal value singular integral of the Hessian matrix of the Newtonian potential convolved with* f.

We note that all entries of the convolution kernel N_{ij} have mean zero on spheres (see e.g. Proposition 2.18 p. 74, [50]) because they are each exact derivatives of ∇N which is homogeneous of degree $1 - d$. Hence the PV integral is well-defined on the Hölder spaces. We also note that the full velocity gradient matrix can be expressed in terms of principal value integrals of the form $PVN_{ij} * \rho$ plus a constant matrix times ρ (see e.g. Prop. 2.17, page 74 [50]). This fact will be used below in estimating ∇v in both sup and Hölder norms.

Next we derive a crude estimate on the size of the support of $\rho(x, t)$:

Lemma 2.3. *Suppose that* ρ_0 *is supported in a ball of radius* R_0. *Then for all* $t \in [0, T)$, $\rho(\cdot, t)$ *is supported in a ball of radius*

$$R(t) = R_0 + \frac{C}{k}(\|\rho_0\|_{L^1} + \|\rho_0\|_{L^\infty})t \tag{2.18}$$

where $C > 0$ *is a constant depending only on the dimension*

Proof. This Lemma is a direct consequence of a simple potential theory estimate that give a bound on the velocity of the particle path:

$$\|v(\cdot,t)\|_{L^\infty} = \|\nabla N * \rho(\cdot,t)\|_{L^\infty} \leq \frac{C}{k}(\|\rho_0\|_{L^1} + \|\rho_0\|_{L^\infty}) \tag{2.19}$$

for some constant C depending only on the dimension. This potential theory estimate is proven in the next subsection, see (2.40). □

Differentiating the particle equation gives

$$\frac{d}{dt}\nabla_\alpha X(\alpha,t) = \nabla v(X(\alpha,t),t)\nabla_\alpha X(\alpha,t). \tag{2.20}$$

This equation directly implies

$$\frac{d}{dt}\|\nabla_\alpha X(\cdot,t)\|_{L^\infty} \leq \|\nabla v(X(\cdot,t),t)\|_{L^\infty}\|\nabla_\alpha X(\cdot,t)\|_{L^\infty},$$

and hence

$$\|\nabla_\alpha X(\cdot,t)\|_{L^\infty} \leq \exp\left(\int_0^t \|\nabla v(\cdot,s)\|_{L^\infty} dx\right). \tag{2.21}$$

To bound $|\nabla_\alpha X(\cdot,t)|_\gamma$, we note that equation (2.20) implies that

$$\begin{aligned}
&\frac{d}{dt}|\nabla_\alpha X(\cdot,t)|_\gamma && (2.22)\\
&\quad\leq |\nabla v(X(\cdot,t),t)|_\gamma \|\nabla_\alpha X(\cdot,t)\|_{L^\infty} + \|\nabla v(X(\cdot,t),t)\|_{L^\infty}|\nabla_\alpha X(\cdot,t)|_\gamma && (2.23)\\
&\quad\leq |\nabla v(\cdot,t)|_\gamma \|\nabla_\alpha X(\cdot,t)\|_{L^\infty}^{1+\gamma} + \|\nabla v(X(\cdot,t),t)\|_{L^\infty}|\nabla_\alpha X(\cdot,t)|_\gamma && (2.24)\\
&\quad\leq C|\rho(\cdot,t)|_\gamma e^{(1+\gamma)\int_0^t \|\nabla v(\cdot,s)\|_{L^\infty} ds} + \|\nabla v(\cdot,t)\|_{L^\infty}|\nabla_\alpha X(\cdot,t)|_\gamma. && (2.25)
\end{aligned}$$

The last estimate is a direct application of (2.17) and (2.21). Using Lemma (2.1) combined with the fact that the inverse characteristic map satisfies the equation $\frac{d}{dt}X^{-t} = -v(X^{-t},t)$, and thus satisfies an inequality like (2.21), we obtain:

$$|\rho(\cdot,t)|_\gamma \leq \frac{|\rho_0|_\gamma}{k^2}\exp\left(\gamma\int_0^t \|\nabla v(\cdot,s)\|_{L^\infty} ds\right). \tag{2.26}$$

Finally applying (2.16) with $\epsilon = (\|\rho(\cdot,t)\|_{L^\infty}/|\rho(\cdot,t)|_\gamma)^{1/\gamma}$ we have

$$\|\nabla v(\cdot,t)\|_{L^\infty} \leq C\left\{\|\rho(\cdot,t)\|_{L^\infty} + \max\left(1, \ln\left(\frac{R(t)|\rho(\cdot,t)|_\gamma^{1/\gamma})}{\|\rho(\cdot,t)\|_{L^\infty}^{1/\gamma}}\right)\|\rho(\cdot,t)\|_{L^\infty}\right)\right\}.$$

Note that due to Lemma (2.3) and (2.13) the logarithm term can be bounded as follow

$$\ln\left(\frac{R(t)|\rho(\cdot,t)|_\gamma^{1/\gamma})}{\|\rho(\cdot,t)\|_{L^\infty}^{1/\gamma}}\right) \leq C + \frac{1}{\gamma}\ln|\rho(\cdot,t)|_\gamma$$

for some constant C which depends only on the initial data ρ_0 and the time T. And therefore, using (2.13) again we find

$$\|\nabla v(\cdot,t)\|_{L^\infty} \leq c_1 + c_2 \ln|\rho(\cdot,t)|_\gamma \tag{2.27}$$

for some constant c_1 and c_2 which depends only on the initial data ρ_0 and the time T. Plugging (2.26) in (2.27) we obtain:

$$\|\nabla v(\cdot,t)\|_{L^\infty} \leq \tilde{c}_1 + \tilde{c}_2 \int_0^t \|\nabla v(\cdot,s)\|_{L^\infty} ds \tag{2.28}$$

where $\tilde{c}_1$ and $\tilde{c}_2$ are again two constants which depend only on the initial data ρ_0 and the time T. By Gronwall lemma this gives us a bound for $\|\nabla v(\cdot,t)\|_{L^\infty}$ on the time interval $[0,T)$, which in turn, from (2.26), gives a bound for $|\rho(\cdot,t)|_\gamma$ on the same time interval $[0,T)$. We can then use these two bounds on $\|\nabla v(\cdot,t)\|_{L^\infty}$ and $|\rho(\cdot,t)|_\gamma$ together with Gronwall lemma to conclude from (2.25) that $|\nabla_\alpha X^t|_\gamma$ is bounded on the time interval $[0,T)$.

Similar but easier estimates can be obtained for the other terms in the Banach norm $\|X^t\|_{1,\gamma}$ defined in (2.3). This concludes the proof of Theorem (2.2).

2.2. *Existence of L^∞ solutions*

This subsection is devoted to the proof of the following theorem:

Theorem 2.3. *Let $\rho_0 \in L^1 \cap L^\infty(\mathbb{R}^d)$ with compact support and let T be such that:*

$$0 < T < \frac{1}{|\rho_0|_{max}}. \tag{2.29}$$

Then there exists a function

$$\rho \in C([0,T], L^1(\mathbb{R}^d)) \cap L^\infty(\mathbb{R}^d \times (0,T))$$

satisfying equation (1.1) *in the sense of distribution and satisfying $\rho(\cdot,0) = \rho_0(\cdot)$. Moreover for all $t \in [0,T]$ we have the following equalities:*

$$\int_{\mathbb{R}^d} \rho(x,t)dx = \int_{\mathbb{R}^d} \rho_0(x)dx, \tag{2.30}$$

$$|\rho(\cdot,t)|_{max} = \left(\frac{1}{|\rho_0|_{max}} - t\right)^{-1}, \quad \textit{and} \quad |\rho(\cdot,t)|_{min} = \left(\frac{1}{|\rho_0|_{min}} + t\right)^{-1}. \tag{2.31}$$

Note that if the initial data is negative, then $|\rho_0|_{max} = 0$ and T can be chosen as large as we want. Therefore when the equation is "spreading", we have global existence. We recall that a function $\rho(x,t)$ satify equation (1.1) in the sense of distribution if for all $\phi \in C_0^\infty(\mathbb{R}^d \times (0,T))$,

$$\int_0^T \int_{\mathbb{R}^d} \left(\frac{\partial \phi}{\partial t}(x,t) + v(x,t) \cdot \nabla \phi(x,t)\right) \rho(x,t) dx dt = 0 \tag{2.32}$$

$$\text{where} \quad v(x,t) = -(\nabla N * \rho(\cdot,t))(x). \tag{2.33}$$

Let us introduce the norm

$$|||\cdot||| = \|\cdot\|_{L^1} + \|\cdot\|_{L^\infty}.$$

Since $\rho \in C([0,T], L^1(\mathbb{R}^d)) \cap L^\infty(\mathbb{R}^d \times [0,T])$ we clearly have that

$$|||\rho(\cdot,t)||| \leq C \quad \text{for all } t \in [0,T]$$

and as we will see, from classical potential theory estimates, this implies that the velocity field $v = -\nabla N * \rho$ is bounded on $\mathbb{R}^d \times (0,T)$. Therefore equation (2.32) makes sense.

To prove Theorem 2.3 we follow the ideas in [9,50,65] by approximating the initial data by convolving with a mollifier. As usual let $\eta \in C_0^\infty(\mathbb{R}^d)$ be a positive function of mass 1 and define $\eta^\epsilon(x) = \epsilon^{-d}\eta(x/\epsilon)$.

Proposition 2.1. *Consider a compactly supported initial density $\rho_0 \in L^1 \cap L^\infty(\mathbb{R}^d)$ and let ρ^ϵ, v^ϵ be the corresponding smooth solution of the same evolution equation with regularized initial data $\rho_0^\epsilon := \eta^\epsilon * \rho_0$ on the time interval $[0,T]$ where $T < 1/|\rho_0|_{max}$. Then we have the following:*

(i) $\rho^\epsilon \in C([0,T], L^1(\mathbb{R}^d))$.

(ii) There exists constants $c_1 > 0$ and $c_2 > 0$ such that

$$\|v^\epsilon(\cdot,t)\|_{L^\infty} \leq c_1 |||\rho^\epsilon(\cdot,t)||| \leq c_2 |||\rho_0||| \qquad \text{for all } \epsilon > 0 \text{ and } t \in [0,T].$$

(iii) There exists functions ρ and $v = -\nabla N * \rho$ such that

$$\sup_{t\in[0,T]} \|\rho^\epsilon(\cdot,t) - \rho(\cdot,t)\|_{L^1(\mathbb{R}^d)} \to 0 \qquad \text{as } \epsilon \to 0 \tag{2.34}$$

$$\|v^\epsilon - v\|_{L^\infty(\mathbb{R}^d \times (0,T))} \to 0 \qquad \text{as } \epsilon \to 0. \tag{2.35}$$

Proof. By mollifying the initial data at time zero, we consider continuous solutions of the above problem

$$\rho^\epsilon(x,t) = \frac{\rho_0^\epsilon(X_\epsilon^{-t}(x))}{1 - \rho_0^\epsilon(X_\epsilon^{-t}(x))t}. \tag{2.36}$$

where the particle trajectories satisfy

$$\frac{d}{dt} X_\epsilon^t = v^\epsilon(X_\epsilon^t(\alpha,t),t), \quad X_\epsilon^0(\alpha) = \alpha,$$

and the velocity $v^\epsilon = \nabla N * \rho^\epsilon$. Recall from the previous section that the function $t \mapsto \rho^\epsilon(X_\epsilon^t(\alpha),t)\, \det\nabla_\alpha X_\epsilon^t(\alpha)$ is constant and therefore, using (2.36), we have that

$$\det(\nabla_\alpha X_\epsilon^t(\alpha)) = 1 - \rho_0^\epsilon(\alpha)t. \tag{2.37}$$

As in the previous subsection define the constants $0 < k < 1$ and $K \geq 1$ by

$$k = 1 - T|\rho_0|_{max} \quad \text{and} \quad K = 1 + T|\rho_0|_{min}. \tag{2.38}$$

We have then

$$k \leq \det(\nabla_\alpha X_\epsilon^t(\alpha)) \leq K \tag{2.39}$$

for all $\epsilon > 0$, $t \in [0,T]$ and $\alpha \in \mathbb{R}^d$.

We first prove (ii). Note that using the fact that $\det(\nabla_\alpha X_\epsilon^t(\alpha)) = 1-\rho_0^\epsilon(\alpha)t > 0$ and doing the change of variable $\alpha = X_\epsilon^{-t}(x)$ we have

$$\|\rho^\epsilon(\cdot,t)\|_{L^1} = \int_{\mathbb{R}^d} \frac{|\rho_0^\epsilon(X_\epsilon^{-t}(x))|}{1-\rho_0^\epsilon(X_\epsilon^{-t}(x))t} dx = \int_{\mathbb{R}^d} |\rho_0^\epsilon(\alpha)|\, d\alpha = \|\rho_0^\epsilon\|_{L^1} \leq \|\rho_0\|_{L^1}.$$

From (2.36) we easily obtained $\|\rho^\epsilon(\cdot,t)\|_{L^\infty} \leq \frac{2}{k}\|\rho_0^\epsilon\|_{L^\infty} \leq \frac{2}{k}\|\rho_0\|_{L^\infty}$ for all $t \in [0,T]$ (such an estimate was derived in the previous section, see (2.11)–(2.13)). We therefore obtain

$$|||\rho^\epsilon(\cdot,t)||| \leq \frac{2}{k}|||\rho_0||| \quad \forall t \in [0,T].$$

Now let $\omega(x)$ be the characteristic function of the unit ball, $\omega(x) = \chi_{B(0,1)}(x)$, then:

$$\begin{aligned}\|v^\epsilon(\cdot,t)\|_{L^\infty} &\leq \|\omega\nabla N\|_{L^1}\, \|\rho^\epsilon\|_{L^\infty} + \|(1-\omega)\nabla N\|_{L^\infty}\, \|\rho^\epsilon\|_{L^1} \\ &\leq C|||\rho^\epsilon(\cdot,t)||| \leq \frac{2C}{k}|||\rho_0||| \quad (2.40)\end{aligned}$$

which concludes the proof of (ii).

We now turn to the proof of (iii). We first need the following potential theory estimate that establishes a uniform log-Lipschitz estimate for the velocity field:

Lemma 2.4. *(Potential theory estimate for the velocity) Given an initial density $\rho_0 \in L^1 \cap L^\infty(\mathbb{R}^d)$ and let ρ^ϵ and v^ϵ be the smooth solutions as defined above. Then v^ϵ satisfies the following estimate independent of ϵ*

$$\sup_{t\in[0,T]} |v^\epsilon(x^1,t) - v^\epsilon(x^2,t)| \leq c|||\rho(\cdot,t)||||x^1-x^2|(1-\ln^-|x^1-x^2|), \quad (2.41)$$

where $\ln^-$ is the negative part (near field) of the natural log.

This lemma is proved for the case of the 2D Biot-Savart kernel for the incompressible Euler equations in [50]. The extension to our problem is straightforward because our velocity kernel satisfies the same conditions as the Biot-Savart kernel, in fact the Biot-Savart kernel is a special case of the orthogonal flow in 2D. We leave the proof to the reader, noting that the estimate is well-known for potential theory in $\mathbb{R}^d$ for the Poisson equation. This lemma directly yields the following estimates for the particle paths:

Lemma 2.5. *(Potential theory estimates for characteristics) Given the assumptions of Lemma 2.4 then there exists $C > 0$ and an exponent $\beta(t) = \exp(-C|||\rho_0|||t)$ such that for all $\epsilon > 0$ and $t \in [0,T]$,*

$$|X_\epsilon^{-t}(x^1) - X_\epsilon^{-t}(x^2)| \leq C|x^1-x^2|^{\beta(t)} \quad (2.42)$$

$$|X_\epsilon^{t}(\alpha^1) - X_\epsilon^{t}(\alpha^2)| \leq C|\alpha^1-\alpha^2|^{\beta(t)} \quad (2.43)$$

and for all $t_1, t_2 \in [0,T]$,

$$|X_\epsilon^{-t_1}(x) - X_\epsilon^{-t_2}(x)| \leq C|t_1-t_2|^{\beta(t)} \quad (2.44)$$

$$|X_\epsilon^{t_1}(\alpha) - X_\epsilon^{t_2}(\alpha)| \leq C|t_1-t_2|^{\beta(t)}. \quad (2.45)$$

This lemma is proved in [50] (see Lemma 8.2) assuming the conditions of Lemma 2.4 above. We note that the a priori bound for the L^∞ norm of the velocity field actually gives Lipschitz continuity in time, although this is not needed for the proof below. By the Arzelà-Ascoli theorem there exists two functions $X^t(\alpha)$ and $Y^t(x)$ and a sequence $\epsilon_k \to 0$ such that

$$X^t_{\epsilon_k}(\alpha) \to X^t(\alpha) \quad \text{and} \quad X^{-t}_{\epsilon_k}(x) \to Y^t(x) \qquad \text{as } \epsilon_k \to 0 \tag{2.46}$$

and these convergences are uniform both in time and space on compact set of $\mathbb{R}^d \times [0,T]$. By passing to the limit in

$$X^t_\epsilon(X^{-t}_\epsilon(x)) = x; \quad X^{-t}_\epsilon(X^t_\epsilon(\alpha)) = \alpha$$

we obtain that Y^t is the inverse of X^t. So we will write $Y^t = X^{-t}$.

Given the above limiting particle paths $X^{-t}(x)$ we define the limiting density according to the formula

$$\rho(x,t) = \frac{\rho_0(X^{-t}(x))}{1-\rho_0(X^{-t}(x))t}. \tag{2.47}$$

We also define the functions

$$\tilde{\rho}^\epsilon_0(\alpha,t) \equiv \frac{\rho^\epsilon_0(\alpha)}{1-\rho^\epsilon_0(\alpha)t} \quad \text{and} \quad \tilde{\rho}_0(\alpha,t) \equiv \frac{\rho_0(\alpha)}{1-\rho_0(\alpha)t}$$

so that ρ^ϵ and ρ can be rewritten as:

$$\rho^\epsilon(x,t) = \tilde{\rho}^\epsilon_0(X^{-t}_\epsilon(x),t) \quad \text{and} \quad \rho(x,t) = \tilde{\rho}_0(X^{-t}(x),t). \tag{2.48}$$

The tilde notation is used to denote the time evolving densities in Lagrangian coordinates. Our goal next is to prove that ρ^ϵ converge in L^1 uniformly in time toward ρ. The proof here differs from the arguments in [50] for the 2D vorticity problem due to the fact that the particle paths are not volume preserving, in contrast to the incompressibility of the 2D vorticity problem, and the fact that the density evolves in a prescribed way along particle paths rather than being conserved. We first derive some straightforward estimates on $\tilde{\rho}^\epsilon_0$ and $\tilde{\rho}_0$:

Lemma 2.6. *For all $\epsilon > 0$ and $t, s \in [0,T]$ we have:*

$$\sup_{t\in[0,T]} \|\tilde{\rho}^\epsilon_0(\cdot,t) - \tilde{\rho}_0(\cdot,t)\|_{L^1} \le \frac{1}{k^2}\|\rho^\epsilon_0(\cdot) - \rho_0(\cdot)\|_{L^1}, \tag{2.49}$$

$$\|\tilde{\rho}^\epsilon_0(\cdot,t) - \tilde{\rho}^\epsilon_0(\cdot,s)\|_{L^1} \le \frac{\|\rho_0\|_{L^\infty}\|\rho_0\|_{L^1}}{k^2}\,|t-s|\,, \tag{2.50}$$

$$\|\nabla_\alpha \tilde{\rho}^\epsilon_0(\cdot,t)\|_{L^\infty} = \frac{1}{k^2}\|\nabla_\alpha \rho^\epsilon_0(\cdot)\|_{L^\infty}. \tag{2.51}$$

Proof. Estimate (2.49) is a simple consequence of the fact that:

$$\frac{\rho^\epsilon_0(\alpha)}{1-\rho^\epsilon_0(\alpha)t} - \frac{\rho_0(\alpha)}{1-\rho_0(\alpha)t} = \frac{\rho^\epsilon_0(\alpha)-\rho_0(\alpha)}{(1-\rho^\epsilon_0(\alpha)t)(1-\rho_0(\alpha)t)}.$$

Estimate (2.50) come from the equality

$$\frac{\rho_0^\epsilon(\alpha)}{1-\rho_0^\epsilon(\alpha)t} - \frac{\rho_0^\epsilon(\alpha)}{1-\rho_0^\epsilon(\alpha)s} = \frac{\rho_0^\epsilon(\alpha)^2}{(1-\rho_0^\epsilon(\alpha)t)(1-\rho_0^\epsilon(\alpha)s)}(t-s).$$

Estimate (2.51) comes from the fact that:

$$\nabla_\alpha \tilde{\rho}_0^\epsilon(\alpha,t) = \frac{1}{(1-\rho_0^\epsilon(\alpha)t)^2}\nabla_\alpha \rho_0^\epsilon(\alpha). \qquad \square$$

Then we note that as a direct consequence of (2.39) and the change of variable formula, we have that for any nonnegative integrable function f,

$$k\int_{\mathbb{R}^d} f(\alpha)d\alpha \le \int_{\mathbb{R}^d} f(X_\epsilon^{-t}(x))dx \le K\int_{\mathbb{R}^d} f(\alpha)d\alpha. \tag{2.52}$$

To conclude the proof of (iii) we will need a similar estimate for the limiting particle path $X^{-t}(x)$:

Lemma 2.7. *For all $t\in[0,T]$, and nonnegative $f\in L^1(\mathbb{R}^d)$,*

$$\int_{\mathbb{R}^d} f(X^{-t}(x))dx \le K\int_{\mathbb{R}^d} f(\alpha)d\alpha. \tag{2.53}$$

The proof, which involves some technical arguments from real analysis, can be found in the appendix. We are now ready to prove that ρ^ϵ converge in L^1 uniformly in time toward ρ. Using formula (2.48) we write:

$$\|\rho^\epsilon(\cdot,t)-\rho(\cdot,t)\|_{L^1} \le \|\tilde{\rho}_0^\epsilon(X_\epsilon^{-t},t)-\tilde{\rho}_0(X_\epsilon^{-t},t)\|_{L^1} + \|\tilde{\rho}_0(X_\epsilon^{-t},t)-\tilde{\rho}_0(X^{-t},t)\|_{L^1}.$$

Using (2.52) and (2.49) we see that the first term is bounded by $\frac{K}{k^2}\|\rho_0^\epsilon-\rho_0\|_{L^1}$ and therefore can be made small uniformly in time. Next we rewrite the second term as

$$\begin{aligned}\|\tilde{\rho}_0(X_\epsilon^{-t},t)-\tilde{\rho}_0(X^{-t},t)\|_{L^1} &\le \|\tilde{\rho}_0(X_\epsilon^{-t},t)-\tilde{\rho}_0^{\epsilon_1}(X_\epsilon^{-t},t)\|_{L^1}\\ &\quad + \|\tilde{\rho}_0^{\epsilon_1}(X_\epsilon^{-t},t)-\tilde{\rho}_0^{\epsilon_1}(X^{-t},t)\|_{L^1} + \|\tilde{\rho}_0^{\epsilon_1}(X^{-t},t)-\tilde{\rho}_0(X^{-t},t)\|_{L^1}.\end{aligned}$$

Note that the function $\tilde{\rho}^{\epsilon_1}$ is different than $\tilde{\rho}^\epsilon$. Let us fix a $\delta>0$. Once again, because of the bound (2.52) and the bound (2.53) from Lemma 2.7 we can choose an ϵ_1 such that the first and the last term are smaller than $\delta/3$ for all $\epsilon>0$ and for all $t\in[0,T]$. We then claim that as $\epsilon\to 0$, the middle term converge to 0 uniformly in time. Indeed, because of (2.51), there exists a constant $C(\epsilon_1)>0$ such that

$$|\tilde{\rho}_0^{\epsilon_1}(X_\epsilon^{-t}(x),t)-\tilde{\rho}_0^{\epsilon_1}(X^{-t}(x),t)| \le C(\epsilon_1)|X_\epsilon^{-t}(x)-X^{-t}(x)|.$$

Using the uniform convergence of the backward particle path and the fact that there exists a compact set K_0 such that

$$X_\epsilon^t(\mathrm{supp}\rho_0^{\epsilon_1}) \subset K_0 \quad \text{for all } t\in[0,T] \text{ and all } \epsilon>0,$$

we can then choose ϵ small enough to make the $\|\tilde{\rho}_0^{\epsilon_1}(X_\epsilon^{-t},t)-\tilde{\rho}_0^{\epsilon_1}(X^{-t},t)\|_{L^1}$ less than $\delta/3$ for all $t\in[0,T]$. This conclude the proof of (2.34).

We now show (2.35). The proof follows [50]. Let $\omega_\delta(x)$ be the characteristic function of the ball of radius δ, $\omega_\delta(x) = \chi_{B(0,\delta)}(x)$, then:

$$\begin{aligned}\|v^\epsilon(\cdot,t) - v(\cdot,t)\|_{L^\infty} &\leq \|\omega_\delta \nabla N\|_{L^1}(\|\rho^\epsilon - \rho\|_{L^\infty}) + \|(1-\omega_\delta)\nabla N\|_{L^\infty}\ \|\rho^\epsilon - \rho\|_{L^1} \\ &\leq \|\omega_\delta \nabla N\|_{L^1} \frac{2\|\rho_0\|_{L^\infty}}{k} + \|(1-\omega_\delta)\nabla N\|_{L^\infty}\ \|\rho^\epsilon - \rho\|_{L^1}\end{aligned}$$

where we have used the bounds $\|\rho^\epsilon(\cdot,t)\|_{L^\infty} \leq \frac{1}{k}\|\rho_0\|_{L^\infty}$ and $\|\rho(\cdot,t)\|_{L^\infty} \leq \frac{1}{k}\|\rho_0\|_{L^\infty}$ which can be directly read from the explicit formulas (2.36) and (2.47). Since ∇N is locally integrable the first term can be made small by choosing δ small. Then we let ϵ go to zero and we use the fact that ρ^ϵ converges to ρ strongly in L^1 and uniformly in time. This concludes the proof of (iii).

Finally we show (i). Using formula (2.48) we write:

$$\|\rho^\epsilon(\cdot,t) - \rho^\epsilon(\cdot,s)\|_{L^1} \leq \|\tilde\rho_0^\epsilon(X_\epsilon^{-t},t) - \tilde\rho_0^\epsilon(X_\epsilon^{-t},s)\|_{L^1} + \|\tilde\rho_0^\epsilon(X_\epsilon^{-t},s) - \tilde\rho_0^\epsilon(X_\epsilon^{-s},s)\|_{L^1}$$

and we conclude using (2.52) and (2.50) for the first term, and (2.51) and (2.44) for the second term. The proof of Proposition 2.1 is completed.

We now prove Theorem 2.3:

Proof. [Proof of the Theorem 2.3] Convergences (iii) and bounds (ii) allow to pass to the limit in (2.32)–(2.33) and therefore prove the existence of bounded compactly supported solutions. The uniform convergence (2.34) together with (i) give the continuity of $\rho(t)$ as a function taking values in $L^1(\mathbb{R}^d)$. To prove conservation of mass (2.30), choose the test function ϕ in (2.32) to be

$$\phi(x,t) = \chi^\epsilon_{[t_1,t_2]}(t)\ \chi^\epsilon_{B(0,R)}(x)$$

where $0 < t_1 < t_2 < T$ and R is large enough so that supp $\rho(\cdot,t) \subset B(0,R)$ for all $t \in [0,T]$. The smooth function $\chi^\epsilon_{[t_1,t_2]}$ is equal to one inside $[t_1+\epsilon, t_2-\epsilon]$, equal to zero outside of $[t_1-\epsilon, t_2+\epsilon]$, increasing on $[t_1-\epsilon, t_1+\epsilon]$ and decreasing on $[t_2-\epsilon, t_2+\epsilon]$. The function $\chi^\epsilon_{B(0,R)}$ is similarly defined. Then letting ϵ go to zero in (2.32) and using the fact that

$$t \mapsto \int_{\mathbb{R}^d} \rho(x,t)dt \tag{2.54}$$

is continuous on $[0,T]$ we obtain that

$$\int_{\mathbb{R}^d} \rho(x,t_1)dt = \int_{\mathbb{R}^d} \rho(x,t_2)dt \qquad \text{for all } 0 < t_1 < t_2 < T.$$

Using again (2.54) we can let $t_1 \to 0$ to obtain the desired result. Equalities (2.31) can directly be read from (2.47) together with the fact that for t fixed, the function $f(z) = (1/z - t)^{-1}$ is increasing on $(-\infty, +\infty)$. □

2.3. *Uniqueness of L^∞ solution*

Uniqueness of solutions follows by an energy estimate involving the primitive of ρ - or in other words an H^{-1} inner product for a comparison of two densities. The argument requires several steps and involves some estimates with singular integral operators. It is the same argument that was used in [65] for the classical vorticity problem and more recently in a number of papers for the aggregation problem with and without diffusion, see [56,9,4,58].

Theorem 2.4. *The solution from Theorem 2.3 is unique.*

We omit the proof because it has already been done in a number of references above. We note that several papers already prove partial existence results combined with uniqueness. The main contribution of our paper is to fully develop the sharp existence theory for signed data.

3. Convergence to self-similarity and estimate of the size of the support

In this section we consider solutions of equation (1.1) with negative initial data, or equivalently, solutions of

$$\frac{\partial \rho}{\partial t} + \operatorname{div}(\rho v) = 0, \quad v = \nabla N * \rho \tag{3.1}$$

with positive initial data (note the change of sign in the formula defining the velocity). Recall that for this problem solutions are spreading and exist globally in time, see Theorem 2.3. We prove in the theorem below that any positive solution of (3.1) with initial data in L^∞ and with compact support converges in L^1 to a spreading circular patch. The proof relies on an estimate for all time t of the size of the support of $\rho(\cdot, t)$. For simplicity we normalize everything to mass one and we consider solutions belonging to $\mathcal{P}(\mathbb{R}^d)$, the space of probability measures.

Theorem 3.1. *Suppose $\rho_0 \in \mathcal{P}(\mathbb{R}^d)$ is compactly supported and belongs to $L^\infty(\mathbb{R}^d)$. Choose r_0 and h_0 such that*

$$\text{supp } \rho_0 \subset \overline{B(0, r_0)} \quad \text{and} \quad \|\rho_0\|_{L^\infty} \le h_0. \tag{3.2}$$

Let $\Phi(x,t)$ be the circular patch of mass 1 with initial height h_0, that is

$$\Phi(x,t) = \frac{h_0}{1 + h_0 t}\, \chi_{B(0,R(t))}(x)$$
$$\text{where} \quad R(t) = R_0 \left(1 + h_0 t\right)^{1/d} \quad \text{and} \quad R_0 = (\omega_d h_0)^{-1/d}.$$

Note that since $\rho \in \mathcal{P}(\mathbb{R}^d)$ we necessarily have $R_0 \le r_0$. Define

$$E(t) = \frac{E_0}{(1 + h_0 t)^{1/2^{d-1}}} \quad \text{where} \quad E_0 = \frac{r_0^d}{R_0^d} - 1 \ge 0.$$

Let $\rho(x,t)$ be a solution of the PDE (3.1) *with initial data $\rho_0(x)$. Then for all $t \geq 0$ we have:*

$$\text{supp } \rho(\cdot,t) \subset \overline{B(0,r(t))} \quad \text{where} \quad r(t) = R(t)(1+E(t))^{1/d} \tag{3.3}$$

$$\text{and} \qquad \|\rho(\cdot,t) - \Phi(\cdot,t)\|_{L^1} \leq 2E(t) \tag{3.4}$$

Remark 3.1. We prove in Theorem 4.2 in the next section that in the two dimensional case, the above $1/\sqrt{t}$ convergence rate is sharp (this is done by computing a family of exact elliptical solutions). Moreover, for the special case of radially symmetric data, one has the sharper rate of convergence $1/t$ in all dimensions, because equations reduce to a version of the inviscid Burgers equation (see the last section of [11]).

Remark 3.2. Let us first show that the L^1-estimate (3.4) is a direct consequence of the estimate of the size of the support (3.3). Clearly $\rho(\cdot,t)$ is smaller than $\Phi(\cdot,t)$ inside the ball of radius $R(t)$ and greater outside. Using moreover the fact both $\Phi(\cdot,t)$ and $\rho(\cdot,t)$ have mass 1 we easily find that

$$\begin{aligned}\|\Phi(\cdot,t) - \rho(\cdot,t)\|_{L^1} &= \int_{|x|\leq R(t)} \Phi(x,t) - \rho(x,t)dx + \int_{|x|>R(t)} \rho(x,t)dx \\ &= 1 - \int_{|x|\leq R(t)} \rho(x,t)dx + \int_{|x|>R(t)} \rho(x,t)dx = 2\int_{|x|>R(t)} \rho(x,t)dx.\end{aligned}$$

Using (3.3) and the fact that

$$\|\rho(\cdot,t)\|_{L^\infty} \leq \frac{h_0}{1+h_0 t} = \frac{1}{\omega_d R(t)^d}$$

it is then easy to see that the mass of $\rho(\cdot,t)$ outside of the ball of radius $R(t)$ is bounded by $E(t)$:

$$\begin{aligned}\int_{|x|>R(t)} \rho(x,t)dx = \int_{r(t)\geq|x|>R(t)} \rho(x,t)dx &\leq \int_{r(t)\geq|x|>R(t)} \frac{1}{\omega_d R(t)^d}dx \\ &= \frac{r(t)^d}{R(t)^d} - 1 = E(t).\end{aligned}$$

Remark 3.3. It is enough to prove the theorem for the Hölder continuous solution given by Theorem 2.1. Indeed assume that the result of the theorem holds for all compactly supported initial data which are Hölder continuous and assume that we are given non-smooth initial data $\rho_0 \in L^\infty$ satisfying (3.2). Let $\eta(x)$ be a smooth probability measure supported in the ball of radius 1, define $\eta^\epsilon(x) = \epsilon^{-d}\eta(x/\epsilon)$ and $\rho_0^\epsilon = \rho_0 * \eta^\epsilon$. Note that ρ_0^ϵ is still a probability measure. Now fix a $\delta > 0$. For all $0 < \epsilon < \delta$ the function ρ_0^ϵ satisfy

$$\text{supp } \rho_0^\epsilon \subset \overline{B(0,r_0+\delta)} \quad \text{and} \quad \|\rho_0^\epsilon\|_{L^\infty} \leq h_0. \tag{3.5}$$

Let $\rho^\epsilon(x,t)$ be the classical solution given by Theorem 2.1 starting with initial data ρ_0^ϵ, $0 < \epsilon < \delta$. Since we have assumed the result of the theorem holds for these

solutions, from (3.5) we can conclude that

$$\text{supp } \rho^\epsilon(\cdot,t) \subset \overline{B(0,r_\delta(t))} \quad \text{where} \quad r_\delta(t) = R(t)(1+E_\delta(t))^{1/d}$$

for all $0 < \epsilon < \delta$ where $R(t)$ is defined as in the Theorem and $E_\delta(t)$ is defined by replacing r_0 by $r_0 + \delta$. Fix a time t, since the particle path converge uniformly, by letting $\epsilon \to 0$ we obtain

$$\text{supp } \rho(\cdot,t) \subset \overline{B(0,r_\delta(t))} \quad \text{where} \quad r_\delta(t) = R(t)(1+E_\delta(t))^{1/d}.$$

Then by letting $\delta \to 0$ we obtain the desired estimate (3.3). As pointed out in the previous Remark, (3.4) is a direct consequence

The remainder of this section is devoted to the proof of the Theorem. As noted in Remark 3.3 we can assume without loss of generality that ρ_0 is an Hölder continuous, compactly supported, probability measure. From now on let fix such a ρ_0, let also fix r_0, h_0, $\Phi(x,t)$, $R(t)$ and $E(t)$ to be as defined in the Theorem. Finally let $\rho(x,t)$ be the Hölder continuous solution starting with initial data ρ_0.

3.1. *Change of variables*

We now move into the reference frame of $\Phi(x,t)$. We do the change of variable:

$$\tilde{x} = \frac{x}{R(t)} = \frac{x}{R_0(1+h_0t)^{1/d}}, \qquad \tilde{t} = \ln(1+h_0t) \tag{3.6}$$

$$\text{and we define:} \qquad \tilde{\rho}(\tilde{x},\tilde{t}) = R_0^d e^{\tilde{t}}\, \rho\left(R_0 e^{\tilde{t}/d}\tilde{x}, \frac{e^{\tilde{t}}-1}{h_0}\right). \tag{3.7}$$

One can easily check that $\tilde{\rho}(\tilde{x},\tilde{t})$ satisfies

$$\frac{\partial \rho}{\partial t} + \text{div } (\rho v) = 0, \quad v = \omega_d \nabla N * \rho - \frac{x}{d} \tag{3.8}$$

where we have dropped all the tilde in the above equation for better readability. One can also check that since $\rho(x,t) \le \frac{h_0}{1+h_0t}$ for all $x \in \mathbb{R}^d$ and $t \ge 0$ then

$$\tilde{\rho}(\tilde{x},\tilde{t}) \le \frac{1}{\omega_d} \qquad \text{for all } \tilde{x} \in \mathbb{R}^d \text{ and } \tilde{t} \ge 0. \tag{3.9}$$

Note that the stationary state of (3.8) is the radially symmetric patch of radius one, height $1/\omega_d$ and mass one. Going back to the original variable this stationary state obviously corresponds to $\Phi(x,t)$.

3.2. *Estimate of the size of the support*

In this subsection we drop the tilde for convenience. The following general Lemma is fundamental to our proof:

Lemma 3.1 (Frozen in time estimate of the velocity at the boundary). *Suppose $\mu \in \mathcal{P}(\mathbb{R}^d)$ satisfies*

$$\textit{supp } \mu \subset \overline{B(0,r)} \quad \textit{and} \quad \|\mu\|_{L^\infty} \le \frac{1}{\omega_d} \tag{3.10}$$

for some $r > 0$ (note that since $\mu \in \mathcal{P}(\mathbb{R}^d)$ we necessarily have $r \geq 1$). Then the velocity field

$$v(x) = \omega_d(\nabla N * \mu)(x) - \frac{x}{d}$$

satisfies

$$v(x) \cdot x \leq -\frac{1}{2^{d-1}dr^{d-2}}(r^d - 1) \qquad \text{for all } x \in \partial B(0,r). \tag{3.11}$$

Proof. Choose x such that $|x| = r$. Using the fact that $\nabla N * \chi_{B(0,r)}(x) = x/d$ we obtain

$$v(x) = -\omega_d \, \nabla N * \left[\frac{1}{\omega_d}\chi_{B(0,r)} - \mu\right](x).$$

Note that the function between square bracket is positive and has mass $r^d - 1$ and is supported in $B(0,r)$. So

$$\begin{aligned} v(x) \cdot x = -\omega_d \int_{B(0,r)} \nabla N(x-y) \cdot x \left[\frac{1}{\omega_d} - \mu\right](y)dy \\ \leq -\omega_d \left(\inf_{y \in B(0,r)} \nabla N(x-y) \cdot x\right)\left(r^d - 1\right). \end{aligned}$$

Note that since $|x| \geq |y|$ we have that

$$|x-y|^2 = |x|^2 - 2x \cdot y + |y|^2 \leq 2|x|^2 - 2x \cdot y = 2(x-y) \cdot x$$

Therefore

$$\nabla N(x-y) \cdot x = \frac{(x-y) \cdot x}{d\,\omega_d \|x-y\|^d} \geq \frac{1}{2d\,\omega_d \|x-y\|^{d-2}} \geq \frac{1}{2d\,\omega_d (2r)^{d-2}} \tag{3.12}$$

which conclude the proof. □

Define

$$\Omega_t = \operatorname{supp} \rho(\cdot, t) \quad \text{and} \quad L(t) = \sup_{x \in \Omega_t} |x|. \tag{3.13}$$

Also let $X(\alpha, t)$ be the (rescaled) particle paths, i.e.

$$\frac{d}{dt}X(\alpha,t) = v(X(\alpha,t),t), \quad X(\alpha,0) = \alpha, \tag{3.14}$$

$$\text{where} \quad v(x,t) = \omega_d(\nabla N * \rho(t))(x) - \frac{x}{d}. \tag{3.15}$$

Fix a time $t \geq 0$ and choose α so that $X(\alpha,t) \in \Omega_t$ and $|X(\alpha,t)| = L(t)$. Then, heuristically,

$$\begin{aligned} \frac{d}{dt}\frac{1}{2}L(t)^2 = \frac{d}{dt}\frac{1}{2}|X(\alpha,t)|^2 = \dot{X}(\alpha,t) \cdot X(\alpha,t) \\ = v(X(\alpha,t),t) \cdot X(\alpha,t) \leq -\frac{1}{2^{d-1}d\,L(t)^{d-2}}(L(t)^d - 1) \end{aligned} \tag{3.16}$$

where we have use Lemma 3.1 to obtain the last inequality. Multiplying both side by $d\, L(t)^{d-2}$ leads to

$$\frac{d}{dt}L(t)^d \leq -\frac{1}{2^{d-1}}(L(t)^d - 1)$$

which provide us with an estimate on the size of the support. In order to make the above heuristic argument into a rigorous one, we will need the following amount of regularity on the particle paths:

(i) The particle paths $X(\alpha, t)$ are differentiable in time and satisfy (3.14) pointwise.
(ii) $|v(x,t)|$ is bounded on any compact set of $\mathbb{R}^d \times [0, +\infty)$.

An elementary argument shows that condition (ii) guaranties that $L(t)$ is continuous. Since we have choosen ρ_0 to be Hölder continuous, Section 2 guaranties that the particle paths satisfy the regularity conditions (i) and (ii), see for instance equation (2.19). The above argument is in the same spirit as the proof of finite time blowup for L^∞ solutions of aggregation equations with less singular kernels by the first two authors and Carillo[10], in which they estimate the size of the support of the solution and show it must collapse inside a ball with radius that goes to zero in finite time. We are now ready to prove rigorously the above heuristic argument.

Lemma 3.2 (Estimate of the size of the support). *Let $\rho(x,t)$ be the solution of the rescaled problem* (3.8) *with initial data $\rho_0 \in \mathcal{P}(\mathbb{R}^d) \cap C^\gamma(\mathbb{R}^d)$. Assume that*

$$\textit{supp } \rho_0 \subset \overline{B(0, r_0)} \qquad \textit{and} \qquad \|\rho(\cdot, t)\|_{L^\infty} \leq \frac{1}{\omega_d} \quad \forall t \geq 0. \tag{3.17}$$

Note that since $\rho_0 \in \mathcal{P}(\mathbb{R}^d)$ we necessarily have $r_0 \geq 1$. Let $r(t)$ be such that:

$$\frac{d}{dt}r(t)^d = -\frac{1}{2^{d-1}}(r(t)^d - 1) \quad , \quad r(0) = r_0. \tag{3.18}$$

Then $\rho(\cdot, t)$ is supported in $\overline{B(0, r(t))}$ for all $t \geq 0$.

Proof. Let Ω_t, $L(t)$ and $X(\alpha, t)$ be defined by (3.13) and (3.14). Because $\rho_0 \in C^\gamma$, (i) and (ii) holds and the function $L(t)$ is continuous. For $0 < \epsilon < 1$ define the function $r_\epsilon(t)$ by:

$$\frac{d}{dt}r_\epsilon(t)^d = -\frac{(1-\epsilon)}{2^{d-1}}(r_\epsilon(t)^d - 1) \quad , \quad r_\epsilon(0) = r_0. \tag{3.19}$$

Note that $r_\epsilon(t)$ decays toward 1 slower than the function $r(t)$ defined by (3.18). Note also that for t fixed, $\lim_{\epsilon \to 0} r_\epsilon(t) = r(t)$. We will prove that $\Omega_t \subset \overline{B(0, r_\epsilon(t))}$ for all $t \geq 0$ and all $0 < \epsilon < 1$. Taking the limit as ϵ goes to 0 will then give the desired result. Fix $0 < \epsilon < 1$. We do the proof by contradiction. Assume that there exists a time $t_1 > 0$ such that $L(t_1) > r_\epsilon(t_1)$ and define

$$\mathcal{T} = \{t \geq 0 \,|\, L(t) \geq r_\epsilon(t)\}.$$

Clearly $t_1 \in \mathcal{T}$ so $\mathcal{T}$ is not empty. Since both $L(t)$ and $r_\epsilon(t)$ are continuous the set $\mathcal{T}$ is closed. Therefore there exists a time $t^* \in \mathcal{T}$ such that

$$t^* = \min \mathcal{T}. \tag{3.20}$$

Using again the continuity of $L(t)$ and $r_\epsilon(t)$ we have that $L(t^*) = r_\epsilon(t^*)$. Choose $x \in \Omega_{t^*}$ such that $|x| = L(t^*) = r_\epsilon(t^*)$ and let $\alpha = X^{-t^*}(x)$. For this particle α we have:

$$|X(\alpha, t^*)| = r_\epsilon(t^*) \quad \text{and} \quad |X(\alpha, t)| < r_\epsilon(t) \text{ for all } t < t^*. \tag{3.21}$$

Let us prove the second statement. Since $X(\alpha, t^*) \in \Omega_{t^*}$ then $X(\alpha, t) \in \Omega_t$ for all $t \geq 0$. This simply comes from the fact that $\Omega_t = X^t(\Omega_0)$. Since $X(\alpha, t) \in \Omega_t$ for all $t \geq 0$ we have that $L(t) \geq |X(\alpha, t)|$ for all $t \geq 0$ and therefore it is not possible for $|X(\alpha, t)|$ to become greater or equal to $r_\epsilon(t)$ before time t^* otherwise t^* would not be the min of $\mathcal{T}$. To summarize, $t \mapsto X(\alpha, t)$ is the particle path which first reaches the boundary of the ball of radius $r_\epsilon(t)$ and this occurs at time t^*. Using (3.21) we then get that for $h > 0$,

$$\begin{aligned} \frac{X(\alpha, t^*) - X(\alpha, t^* - h)}{h} \cdot X(\alpha, t^*) &\geq \frac{|X(\alpha, t^*)|^2 - |X(\alpha, t^* - h)||X(\alpha, t^*)|}{h} \\ &\geq \frac{r_\epsilon(t^*) - r_\epsilon(t^* - h)}{h} r_\epsilon(t^*). \end{aligned}$$

Since the particle path are differentiable with respect to time and satisfies (3.14) pointwise (see Section 2), letting $h \to 0$ and then using (3.19) we obtain:

$$\begin{aligned} v(X(\alpha, t^*), t^*) \cdot X(\alpha, t^*) &\geq r'_\epsilon(t^*) r_\epsilon(t^*) \\ &= -\frac{1 - \epsilon}{2^{d-1} d\, r_\epsilon(t^*)^{d-2}} (r_\epsilon(t^*)^d - 1) \\ &> -\frac{1}{2^{d-1} d\, r_\epsilon(t^*)^{d-2}} (r_\epsilon(t^*)^d - 1). \end{aligned}$$

This contradicts Lemma 3.1. □

3.3. *Proof of the theorem*

Let us now put back the tilde. Solving the ODE (3.18) we find that

$$\tilde{r}(\tilde{t})^d - 1 = (\tilde{r}_0^d - 1) e^{-\frac{\tilde{t}}{2^{d-1}}}$$

and going back to the original variable this translates into:

$$\frac{r(t)^d}{R(t)^d} - 1 = \left(\frac{r_0^d}{R_0^d} - 1 \right) \frac{1}{(1 + h_0 t)^{\frac{1}{2^{d-1}}}}.$$

The right-hand side of the above equation is $E(t)$. We therefore have proven estimate (3.3). As pointed out in the Remark 3.2, estimate (3.4) is a direct consequence.

4. Exact solutions and numerical examples

In this section we construct a family of exact solutions in 2D and present numerical results in 2D and 3D. The family of exact solutions consists of elliptical aggregation patches and is derived directly from the well-known theory for elliptical vortex patches. For the collapsing problem, these exact solutions provide us with an example of aggregation patches collapsing to a nontrivial singular measure (Theorem 4.1). For the spreading problem elliptical patches allow us to prove that the convergence rate toward selfsimilarity derived in the previous section is sharp in 2D (Theorem 4.2).

We then present numerical results of more general aggregation patches in 2D and 3D, the latter case having axial symmetry for ease of computation. The numerics can be made very accurate by reformulating the problem as a dynamics equation for the boundary of the patch alone and by doing a time change of variable so that the blow up occurs as $s \to \infty$. The numerics illustrate the phenomena of collapse toward a complex skeleton in the collapsing case (Figures 2, 5 and 6), as well as the phenomena of "pinching" of the boundary in the spreading case (Figures 3 and 7).

4.1. *Elliptical patches in 2D*

There are a class of well-known vortex patch solutions to the 2D Euler equations consisting of rotating ellipses. These are known as the Kirchoff ellipses (see Kirchoff [40] ch. 20, Lamb [41] p. 232, and Majda and Bertozzi [50] ch. 8). For these exact solutions, the velocity field associated with an constant vorticity ellipse can be computed analytically along with the dynamics of the patch. By computing the orthogonal velocity field we immediately obtain an analytical formula for $\nabla N * \rho$ for ρ the characteristic function of an ellipse.

Given a density $\rho = \rho_0 \chi_{E(a,b)}$ where

$$E(a,b) = \left\{ x \middle| \frac{x_1^2}{a^2} + \frac{x_2^2}{b^2} < 1 \right\},$$

the velocity field generated is precisely

$$v(x) = \begin{cases} -\frac{\rho_0}{a+b}(bx_1, ax_2) & x \in E(a,b), \\ -\frac{\rho_0}{\sqrt{a^2+\lambda^2}+\sqrt{b^2+\lambda^2}}((\sqrt{b^2+\lambda})x_1, (\sqrt{a^2+\lambda})x_2) & x \notin E(a,b), \end{cases}$$

where $\lambda(x)$ satisfies

$$\frac{x_1^2}{a^2+\lambda} + \frac{x_2^2}{b^2+\lambda} < 1.$$

We note that inside the ellipse (and on the boundary) the flow field is linear. Linear flow fields map ellipses to ellipses and thus the elliptical shape is preserved under the flow, although the major and minor axes will change. For the vorticity problem this results in exact solutions that rotate at a constant angular velocity. For the aggregation problem it results in ellipses that collapse or spread and for which we obtain explicit ODEs for the major and minor axes:

$$\dot{a} = \dot{b} = -\frac{\rho(t)ab}{a+b}, \quad \rho(t) = \frac{\rho_0}{1-\rho_0 t}.$$

So the quantity $a - b$ is conserved and we obtain the following Theorem about collapsing elliptical patches:

Theorem 4.1. *(Collapse of positive Elliptical Patches toward singular measures) Let $\rho(x,t)$ be the solution of (1.1) starting with initial $\rho_0 \in \mathcal{P}(\mathbb{R}^2)$ being the uniform distribution on the ellipse $E_0 = \left\{ x \,\middle|\, \frac{x_1}{a_0^2} + \frac{x_2}{b_0^2} < 1 \right\}$, $0 < b_0 \leq a_0$. As $t \to T^*$, where $T^* = (\pi a_0 b_0)^{-1}$ is the maximal time of existence, the solution converges weakly-* as a measure toward the weighted distribution on the segment*

$$\mu(x_1) = \frac{2\sqrt{x_0^2 - x_1^2}}{\pi x_0^2} \delta_{I(x_0)}$$

where $\delta_{I(x_0)}$ is the uniform measure on the interval $x_1 \in [-x_0, x_0]$ and $x_0 \equiv a_0 - b_0$ is the semi-major axis of the limiting ellipse, i.e. $a_0 \to x_0$ as $t \to T^*$.

The proof of this theorem is straightforward. From the exact solution we have $b_0 \to 0$ and $a_0 \to x_0$ as $t \to T^*$. Clearly the limiting measure is a weighted measure on the interval from $[-x_0, x_0]$. So what is left is to compute the weight. We note that prior to the collapse the x_2 coordinate of the ellipse boundary satisfies $x_2(x_1) = \pm b(t)\sqrt{1 - \frac{x_1^2}{a(t)^2}}$. The weight function is the limit of the portion of mass that collapses onto the point x on the interval and this is simply $\lim_{t\to T^*} 2\rho(t)x_2(x_1) = \lim_{t\to T^*} 2\rho(t)b(t)\sqrt{1 - \frac{x_1^2}{a(t)^2}}$. Using the fact that $\rho(t) = 1/\pi(a(t)b(t))$ we can substitute this into the limit to obtain that the weight is

$$\lim_{t\to T^*} \frac{2}{\pi a(t)} \sqrt{1 - \frac{x_1^2}{a(t)^2}} = \frac{2}{\pi x_0} \sqrt{1 - \frac{x_1^2}{x_0^2}}.$$

Note also that one can directly integrate the ODEs for a and b, in particular using the dynamics of the product ab. It is easy to solve for both variables:

$$a(t) = \frac{(a_0 - b_0) + \sqrt{(a_0 - b_0)^2 + 4a_0 b_0(1 - \rho_0 t)}}{2}, \tag{4.1}$$

$$b(t) = \frac{-(a_0 - b_0) + \sqrt{(a_0 - b_0)^2 + 4a_0 b_0(1 - \rho_0 t)}}{2}. \tag{4.2}$$

Using the above exact solution we can now prove that the convergence rate in Theorem 3.1 is sharp in two space dimensions.

Theorem 4.2. *(L^1 convergence rate of negative Elliptical Patches toward selfsimilarity) Let $\rho(\cdot,t) = \rho(t)\chi_{E(t)}$ be an elliptical patch solution with negative initial data,*

with $\rho(t) = \frac{-1}{1+t}$ *and* $E(t) = \left\{ x \,\middle|\, \frac{x_1}{a(t)^2} + \frac{x_2}{b(t)^2} < 1 \right\}$, $a(t)$ *and* $b(t)$ *being the semi major axis and semi minor axis of the ellipse* $E(t)$. *Let* $\Phi(x,t) = -(1+t)^{-1}\chi_{B(0,R(t))}$ *where* $R(t) = \sqrt{(1+t)/\pi}$. *Then*

$$\|\rho(\cdot,t) - \Phi(\cdot,t)\|_{L^1} = 4a_0 b_0 \left[2\arctan\left(\sqrt{\frac{a(t)}{b(t)}} \right) - \frac{\pi}{2} \right] = \frac{2\sqrt{a_0 b_0}(a_0 - b_0)}{\sqrt{1+t}} + O\left(\frac{1}{1+t} \right).$$

This is proved by a direct computation involving the above solutions.

Remark 4.1. There are analogous ellipsoid solutions in 3D of the form $\frac{x_1^2}{a^2} + \frac{x_2^2}{b^2} + \frac{x_3^2}{c^2} = 1$ where a, b, c satisfy ODEs involving elliptic integrals. This is due to a known formula for the gradient of the Newtonian potential convolved with an ellipsoid in 3D, a classical result that comes from the Newtonian physics of self-gravitating bodies. Computing these solutions is beyond the scope of this paper however we expect them to have similar qualitative behavior to the 2D elliptical solutions.

4.2. *Collapsing aggregation patches, time rescaling, and contour dynamics*

We now consider the case of a general collapsing patch. Without loss of generality we take the initial density to be one and for simplicity of notation we assume that the patch is simply connected with smooth boundary. Formally we compute a time and amplitude rescaling for the equations of motion by defining

$$s = \ln \frac{1}{1-t}, \quad \tilde{\rho} = (1-t)\rho, \quad \tilde{v} = (1-t)v. \tag{4.3}$$

Plugging these changes into the original equation $\rho_t + \nabla \cdot (\rho v) = 0$, after some calculus we formally obtain

$$\tilde{\rho}_s + \tilde{v} \cdot \nabla \tilde{\rho} = 0; \quad v = -\nabla N * \tilde{\rho} \tag{4.4}$$

where in the above calculation we use the fact that $-\nabla \cdot v = \rho$ and that term cancels the additional term obtained from differentiating $\rho = \frac{\tilde{\rho}}{1-t}$ with respect to time. We also use the fact that $\rho(x,t)$ is $\frac{1}{1-t}$ times the characteristic function of the domain $\Omega_s = \Omega(t)$ for $s = -\ln(1-t)$. The upshot is that we have a new time variable s and the patch singularity occurs as $s \to \infty$. Moreover, the patch remains a characteristic function (the rescaled density does not grow or shrink) and it is simply transported along characteristics of the rescaled velocity. The next step is to rewrite (4.4) as a dynamic equation for the boundary of the patch. This can be done following the classical contour dynamics formulation for vortex patches [66,50]. Note that integrating by parts we can express $\tilde{v}$ as a boundary integral:

$$\tilde{v}(x,s) = -\nabla N * \chi_{\Omega_s}(x) = \int_{\partial\Omega_s} N(x-y) n(y) d\sigma(y). \tag{4.5}$$

For the two dimensional problem, we drop the tilde in equation (4.5) and parametrize the curve $\partial\Omega_s$ by $z(\alpha, s)$, $\alpha \in [0, 2\pi]$, a Lagrangian variable. We obtain

$$v(x,s) = \int_0^{2\pi} N(x - z(\alpha,s)) \Big[\frac{\partial z}{\partial \alpha}(\alpha,s)\Big]^{\perp} d\alpha$$

and since Ω_s moves according to v we get

$$\frac{\partial z}{\partial s}(\alpha,s) = \frac{1}{2\pi}\int_0^{2\pi} \ln|z(\alpha,s) - z(\alpha',s)| \Big[\frac{\partial z}{\partial \alpha}(\alpha',s)\Big]^{\perp} d\alpha'. \tag{4.6}$$

We discretize $\partial\Omega_s$ with N particles $X_1(s), \ldots, X_N(s)$. We use a midpoint rule to approximate the velocity field:

$$\begin{aligned} v(x,s) &= \frac{1}{2\pi}\int_{\partial\Omega_s} \ln|x-y|\, n(y) d\sigma(y) \\ &\approx \frac{1}{2\pi}\sum_{i=1}^{N} \ln\left|x - \frac{X_{i+1}+X_i}{2}\right| \frac{(X_{i+1}-X_i)^{\perp}}{|X_{i+1}-X_i|} |X_{i+1}-X_i| \\ &= \frac{1}{2\pi}\sum_{i=1}^{N} \ln\left|x - \frac{X_{i+1}+X_i}{2}\right| (X_{i+1}-X_i)^{\perp} \end{aligned} \tag{4.7}$$

with the convention that $X_{N+1} := X_1$. See Figure 1a for a graphic explanation of this formula.

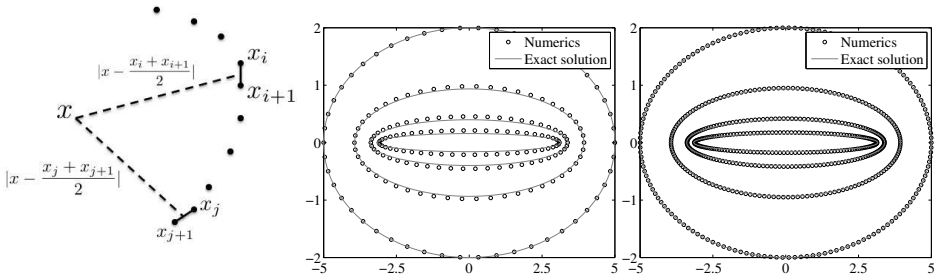

(a) Quadrature schematic (b) Ellipse 50 points (c) Ellipse 150 points

Figure 1: 2D collapsing aggregation patches. (a) schematic of quadrature. Figs. (b) and (c) show an exact elliptical solution with respectively 50 and 150 gridpoints compared with the analytic solution at times $t = 0, 0.62, 0.86, 0.95$.

This leads to the system of ODEs

$$\dot{X_k} = \frac{1}{2\pi}\sum_{i=1}^{N} \ln\left|X_k - \frac{X_{i+1}+X_i}{2}\right| (X_{i+1}-X_i)^{\perp} \quad , \quad 1 \le k \le N \tag{4.8}$$

that we solve using an adaptive Runge-Kutta-Felhberg algorithm order 4/5 ("ODE45" in MATLAB). These schemes use an adaptive timestep chosen by setting the local time truncation error. In our simulations we take that to be smaller than 10^{-5}. Figure 1 (b),(c) show the results of the numerics for the exact elliptical solution starting with the initial ellipse $x_1^2/5^2 + x_2^2/2^2 = 1$. We compare results with 50 vs. 150 grid points at times $t = 0, 0.62, 0.86, 0.95$. The results compare well with the exact solution shown as a solid line. More information about the accuracy of the numerical scheme can be found in the appendix. In Figure 2 we show that aggregation patches of more general shapes typically collapse toward more complex skeletons. Each has initial data that is the characteristic function of some region. The singularity time is $t = 1$. At the collapse time, the patch becomes a singular measure supported on a domain of Lebesgue measure zero which consists of the union of intersecting curves. The patch skeleton shown is actually the solution of true patch at time $t = 0.99995$; the boundary has almost collapsed and the interior is not visible. ca The annulus example in figure 2f retains its empty core at the collapse time.

4.3. *Spreading case in two dimensions*

We now consider the case of a spreading patch solution, corresponding to a negative solution of (1.1) or a positive solution of (3.1). Without loss of generality we assume the initial density is the characteristic function of some region. We make a similar change of variables to those in the previous subsection with some modifications:

$$s = \ln(1+t), \quad \tilde{\rho} = (1+t)\rho, \quad \tilde{v} = (1+t)v - \tilde{x}/d, \quad \tilde{x} = x/(1+t)^{1/d}. \tag{4.9}$$

Note the additional rescaling of space along the lines of the similarity variables described in section 3. Also note that $\tilde{v}$ is divergence free inside the patch, due to the additional x/d term subtracted. Plugging these changes into the original equation $\rho_t + \nabla \cdot (\rho v) = 0$, after some calculus we formally obtain

$$\tilde{\rho}_s + \tilde{v} \cdot \tilde{\nabla}\tilde{\rho} = 0; \quad \tilde{v} = \tilde{\nabla}\tilde{N} * \tilde{\rho} - \tilde{x}/d. \tag{4.10}$$

The patch remains a characteristic function (the rescaled density does not grow or shrink) and it is simply transported along characteristics of the modified velocity field. We write the equation for the boundary of the patch following the contour dynamics formalism described above and compute the solution for several examples in 2D. The results are shown in Figure 3 in the rescaled variables. Note that initial regions of high curvature produce defects in the long time limit in which the boundary folds on itself, despite the L^1 convergence to the exact circular solution. Note that we can not have convergence in L^∞ because the solution and its limit are both piecewise constant. The numerics suggest one may not have pointwise convergence of the boundary due to the defects.

Figure 4 shows a computational example involving interacting particles (point masses) for the spreading problem. Note that they also self-organize in the long time limit to the exact circular patch solution.

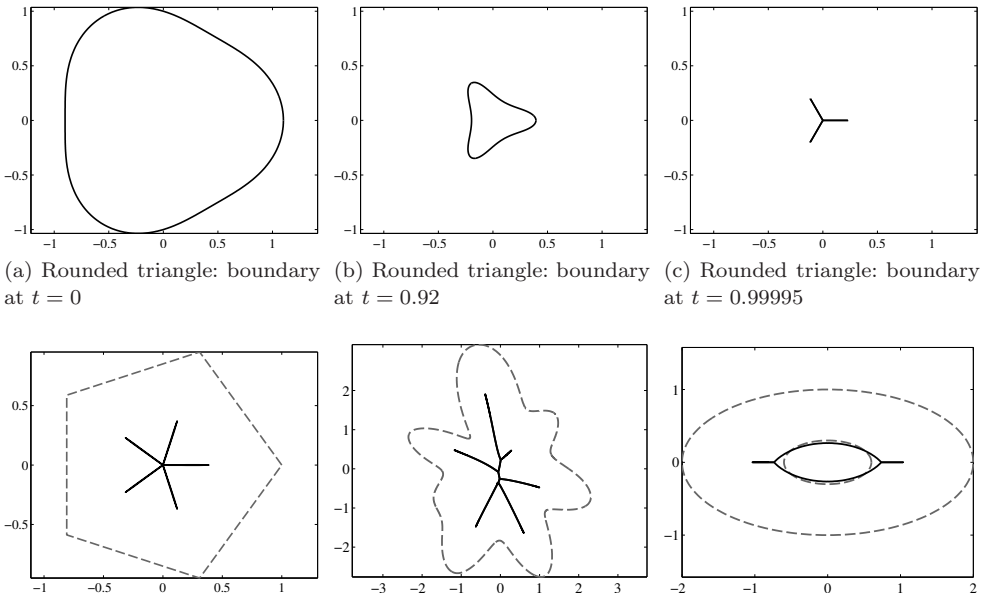

(a) Rounded triangle: boundary at $t = 0$

(b) Rounded triangle: boundary at $t = 0.92$

(c) Rounded triangle: boundary at $t = 0.99995$

(d) A pentagon - 1000 points

(e) A random shape - 5000 points

(f) An annulus - 1000 points

Figure 2: 2D collapsing aggregation patches. All examples show an initial patch that is the characteristic function of some region. At $t = 1$ the solution converges to a set of measure zero. Figures (a)-(c) show snapshots of the boundary evolution of such a patch. In this example, as $t \to 1$, the patch converges toward a singular measure supported on a three branched star. Other high resolution simulations with various shapes are shown in figures (d)-(f). In each image, the dashed line is the boundary of the patch at time $t = 0$ and the solid line is the boundary at time $t = 0.99995$. The number of grid points used us displayed in each subfigure.

4.4. *3D Numerics - axisymmetric patches*

Here we compute some axisymmetric examples in 3D. We construct the boundary of the patch as a surface of revolution. Let

$$\big(x(\alpha), y(\alpha)\big) \in]0, 1[$$

be a curve in the $x - y$ half-plane for $x > 0$. We rotate this curve in three dimensions, about the y-axis, to obtain a surface of revolution. The surface can thus be parametrized by

$$\phi(\alpha, \theta) = \big(x(\alpha)\cos(\theta), y(\alpha), x(\alpha)\sin(\theta)\big), \quad \alpha \in]0, 1[, \, \theta \in]0, 2\pi[.$$

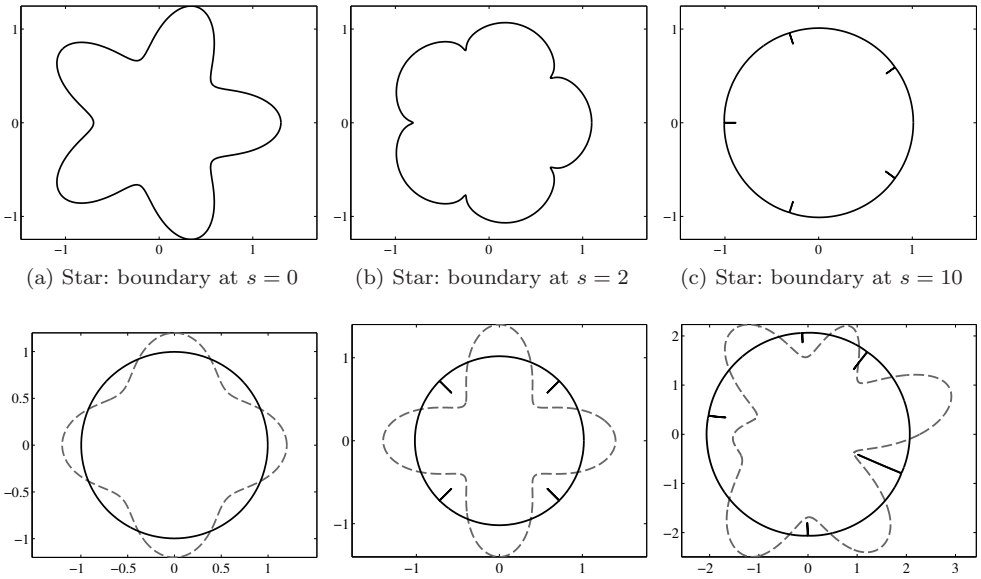

(a) Star: boundary at $s = 0$ (b) Star: boundary at $s = 2$ (c) Star: boundary at $s = 10$

(d) A mildly perturbed circle - 1000 points (e) A strongly perturbed circle - 1000 points (f) A random shape - 5000 points

Figure 3: Four examples of contour dynamics for the rescaled spreading problem (4.10) in two dimensions. Fig. (a)-(c) show snapshots of the boundary evolution of a patch. At time $s = 10$ the patch has reached steady state. Fig. (d)-(f) show various shapes: the initial boundary is shown as a dashed line and the long time limit ($s = 10$) is shown as a solid line.

For the collapsing problem, the velocity at a point p is

$$\vec{v}(p) = \int_\alpha \int_{\theta=0}^{2\pi} -\frac{1}{4\pi\|p - \phi(\alpha,\theta)\|} \frac{\partial \phi}{\partial \theta} \times \frac{\partial \phi}{\partial \alpha}(\alpha,\theta)\, \mathrm{d}\theta \mathrm{d}\alpha.$$

Hence for a point $p = (X, Y, 0)$ in the (Oxy) plane we have

$$\vec{v}(X,Y,0)) = \int_\alpha \int_{\theta=0}^{2\pi} \frac{-x(\alpha) \begin{pmatrix} y'(\alpha)\cos(\theta) \\ -x'(\alpha) \\ y'(\alpha)\sin(\theta) \end{pmatrix}}{4\pi\sqrt{(x(\alpha)\cos(\theta) - X)^2 + (x(\alpha)\sin(\theta))^2 + (y(\alpha) - Y)^2}} \mathrm{d}\theta \mathrm{d}\alpha.$$

By symmetry $\vec{v}(X,Y,0) \cdot \vec{e}_z = 0$ so we define v_X and v_Y by

$$\vec{v}(X,Y,0) = v_X(X,Y)\vec{e}_x + v_Y(X,Y)\vec{e}_y$$

.

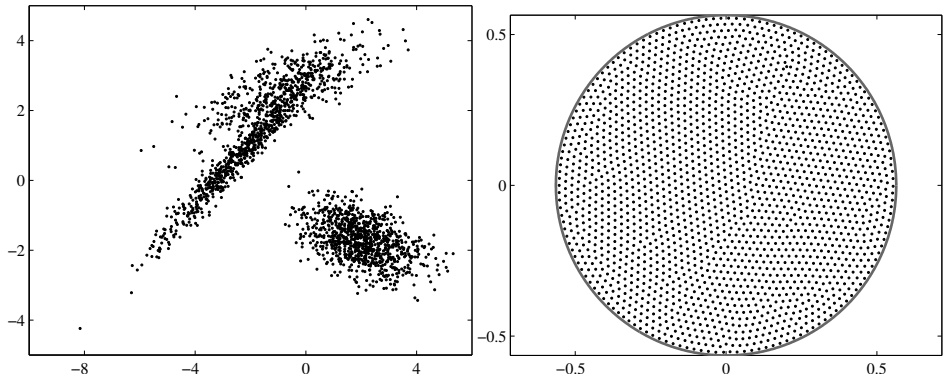

(a) Initial state (b) Final state

Figure 4: 2D spreading dynamics for initial data a sum of 2000 particles. The long time limit is shown on the right.

After some integration we find

$$v_X(X,Y) = \int_\alpha \frac{1}{\pi}\frac{x(\alpha)y'(\alpha)}{A\sqrt{A+B}}\left[(A+B)\mathcal{E}\left(\frac{2A}{A+B}\right) - B\mathcal{F}\left(\frac{2A}{A+B}\right)\right]\mathrm{d}\alpha$$
$$v_Y(X,Y) = \int_\alpha \frac{1}{\pi}\frac{x(\alpha)x'(\alpha)}{\sqrt{A+B}}\mathcal{F}\left(\frac{2A}{A+B}\right)\mathrm{d}\alpha$$

with

$$A(\alpha) = 2x(\alpha)X, \quad B(\alpha) = x^2(\alpha) + X^2 + (y(\alpha) - Y)^2$$

and $\mathcal{E}$, $\mathcal{F}$ are the complete elliptic integral of the first and second kind

$$\mathcal{E}(m) = \int_0^{\frac{\pi}{2}} \sqrt{1 - m\sin^2(x)}\mathrm{d}x, \quad \mathcal{F}(m) = \int_0^{\frac{\pi}{2}} \frac{\mathrm{d}x}{\sqrt{1 - m\sin^2(x)}}, \quad m \in [0,1].$$

If the surface has a toroidal topology then the section in the (Oxy) half-plane is a closed curve Γ. As in the 2D case, we discretize Γ with N particules $(x_1(s), y_1(s)), \ldots, (x_N(s), y_N(s))$ and use a midpoint rule to approximate the velocity field:

$$\dot{x_k} = \frac{1}{\pi}\sum_{i=1}^{N} \frac{x_{i+1}+x_i}{2}(y_{i+1}-y_i)\frac{1}{A_i\sqrt{A_i+B_i}}\left[(A_i+B_i)\mathcal{E}\left(\frac{2A_i}{A_i+B_i}\right) - B_i\mathcal{F}\left(\frac{2A_i}{A_i+B_i}\right)\right]$$
$$\dot{y_k} = \frac{1}{\pi}\sum_{i=1}^{N} \frac{x_{i+1}+x_i}{2}(x_{i+1}-x_i)\frac{1}{\sqrt{A_i+B_i}}\mathcal{F}\left(\frac{2A_i}{A_i+B_i}\right)$$

where $x_{N+1} := x_1, y_{N+1} := y_1$ and

$$A_i = 2x_k \frac{x_{i+1} + x_i}{2},$$
$$B_i = \left(\frac{x_{i+1} + x_i}{2}\right)^2 + x_k^2 + \left(\frac{y_{i+1} + y_i}{2} - y_k\right)^2.$$

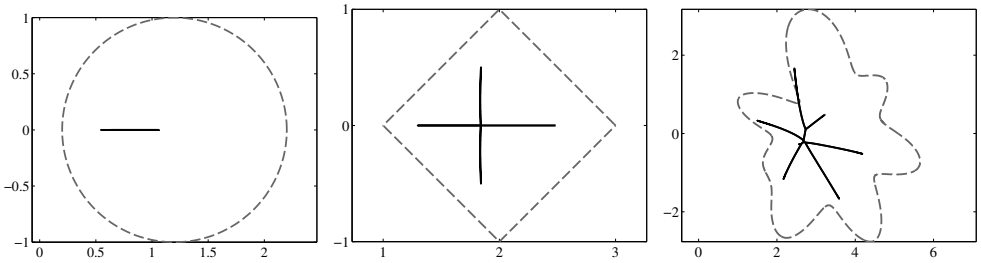

(a) Circle section - 200 points (b) Square section - 600 points (c) Random section - 5000 points

Figure 5: Three examples of 3D collapsing patches showing the section of the surface in the $x - y$ half-plane. Case (b) is also shown below in Figure 6 as a surface of revolution. The dashed line is the initial data and the solid line shows the boundary at $t = 0.99995$.

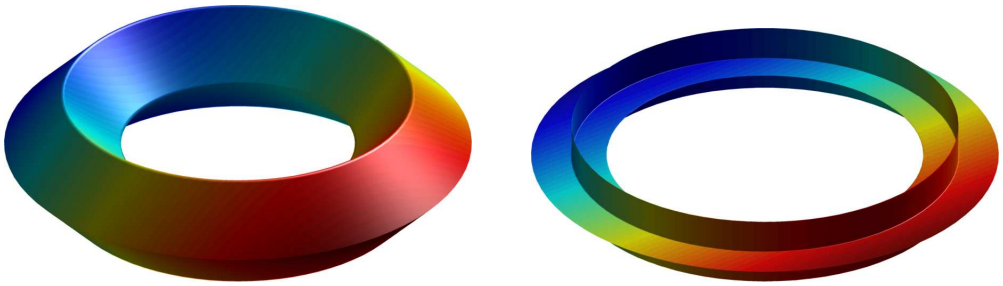

(a) Initial state (b) Collapsed state

Figure 6: 3D visualization of Figure 5b, a toroidal patch with a square section.

As in 2D we present some numerical results. In Figures 5 and 7 we show a section of the surface rather than the surface itself for readability. We also show a complete 3D surface in Figure 6. We observe similar behavior in 2D and in 3D: in the collapsing problem the patches converge to a skeleton of codimension 1, and

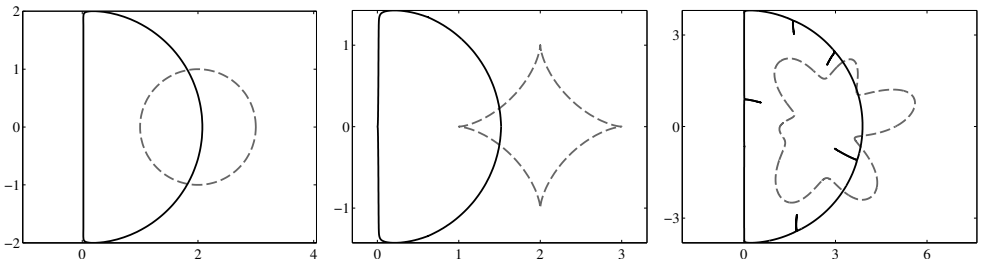

(a) Circle section - 200 points (b) Astroidal section- 400 points (c) Random section- 5000 points

Figure 7: 3D rescaled expanding patches. These figures show the section of the surface in the x–y half-plane. The dashed line is the initial data and the long time limit is shown as a solid line.

in the expanding problem the patches converge to a ball (in rescaled coordinates). Note that in the expanding case, since the figures display the section of the surface in the half plane, the limit is a half circle. Note also that when there is a high curvature the long time limit presents the same defaults on the boundary as in 2D.

Appendix

Proof of Lemma 2.7

Lemma 2.7 *For all $t \in [0,T]$, and nonnegative $f \in L^1(\mathbb{R}^d)$,*

$$\int_{\mathbb{R}^d} f(X^{-t}(x))dx \leq K \int_{\mathbb{R}^d} f(\alpha)d\alpha. \tag{4.11}$$

Proof. Recall that $X_\epsilon^{-t}(x)$ converge uniformly toward $X^{-t}(x)$ on compact subset of $\mathbb{R}^d \times (0,T)$ and that

$$k \leq \det(\nabla_\alpha X_\epsilon^t(\alpha)) \leq K \tag{4.12}$$

for all $\epsilon > 0$, $t \in [0,T]$ and $\alpha \in \mathbb{R}^d$. We are first going to show that

$$\left|X^t(E)\right| \leq K\,|E| \tag{4.13}$$

for all bounded measurable set $E \subset \mathbb{R}^d$. Here $|E|$ denote the Lebesgue measure of the set E.

Assume first that $E = B_{x_0,r}$ is a ball of radius $r < \infty$ centered at $x_0 \in \mathbb{R}^d$. Given any $\lambda > 1$ there exists an $\epsilon > 0$ such that

$$\left|X^t(B_{x_0,r})\right| \leq \left|X_\epsilon^t(B_{x_0,\lambda r})\right| \leq K\,|B_{x_0,\lambda r}| \leq \lambda^d K\,|B_{x_0,r}|\,.$$

To see this, note that since $X_\epsilon^{-t}(x)$ converge uniformly toward $X^{-t}(x)$ on compact sets, we have that given $\lambda > 1$, $X^t(B_{x_0,r}) \subset X_\epsilon^t(B_{x_0,\lambda r})$ if ϵ is small enough. This

give the first inequality. The second inequality comes from (4.12) and the third inequality is just a rescaling of the ball in $\mathbb{R}^d$. Letting $\lambda \to 1$ we see that (4.13) holds for any ball of finite radius.

Assume now that $E = \mathcal{O}$ is a bounded open set and let $\lambda > 1$. By a classical covering lemma (see e.g. Lemma 2, p. 15, in [61]) there exists a finite number of pairwise disjoint balls $B_{x_1,r_1}, \ldots, B_{x_k,r_k}$ so that

$$\cup_i B_{x_i,r_i} \subset \mathcal{O} \subset \cup_i B_{x_i,\lambda r_i}.$$

Then, since (4.13) holds for balls, we have:

$$\left|X^t(\mathcal{O})\right| \leq \sum_i \left|X^t(B_{x_i,\lambda r_i})\right| \leq K \sum_i |B_{x_i,\lambda r_i}| = \lambda^d K \sum_i |B_{x_i,r_i}| \leq \lambda^d K \left|\mathcal{O}\right|.$$

Letting $\lambda \to 1$ we see that (4.13) holds for any bounded open set.

We now show that (4.13) holds for any bounded measurable set E. Let $\mathcal{O}_n$ be a sequence of bounded open set such that $E \subset \mathcal{O}_n$ and $|\mathcal{O}_n| \to |E|$. Thus we have

$$\left|X^t(E)\right| \leq \left|X^t(\mathcal{O}_n)\right| \leq K \left|\mathcal{O}_n\right| \to K \left|E\right|.$$

Finally we approximate f by simple functions. For $\lambda > 1$ let:

$$f \leq \sum_{i=-\infty}^{\infty} \lambda^i \chi_{E_i} < \lambda f, \quad \text{where} \quad E_i = \{x : \ \lambda^{i-1} < f(x) \leq \lambda^i\}.$$

Here $\chi_{E_i}(x)$ is the characteristic function of the set E_i. Using this construction we have

$$\int_{\mathbb{R}^d} f(X^{-t}(x))dx \leq \int_{\mathbb{R}^d} \sum_i \lambda^i \chi_{E_i}(X^{-t}(x))dx = \sum_i \lambda^i \left|X^t(E_i)\right|$$
$$\leq K \sum_i \lambda^i |E_i| = K \int_{\mathbb{R}^d} \sum_i \lambda^i \chi_{E_i}(\alpha)d\alpha \leq \lambda K \int_{\mathbb{R}^d} f(\alpha)d\alpha. \quad \square$$

Numerical convergence in 2D

We perform a mesh refinement study to illustrate that the scheme is $O(\frac{1}{N})$ where N is the number of particles which discretize the boundary of the patch. The quadrature would ordinarily be $O(\frac{1}{N^2})$ however the singularity of the kernel keeps it at $O(\frac{1}{N})$ and this is illustrated below.

We compute the time evolution of an elliptical patch with $N = 2^k N$ particles on the boundary for $k = 1, \ldots, 12$ from time $s = 0$ to time $s = 3$. Then we compare at final time $s = 3$ each solution f_k with $2^k N$ points, $k = 1, \ldots, 11$ to the solution f_{12} that has the most points. More specifically we compute the average distance between the points of f_k and the points of f_{12} (subsampled). Then we repeated the calculation with the non singular kernel $K(x) = e^{-\frac{x^2}{2}}$ instead of the newtonian kernel N. Then we do a linear fit $y = px + q$. Figure 8 displays both results. The slope of the line for the Newtonian kernel is -1.06 whereas the slope of the line for the exponential kernel is -2.02.

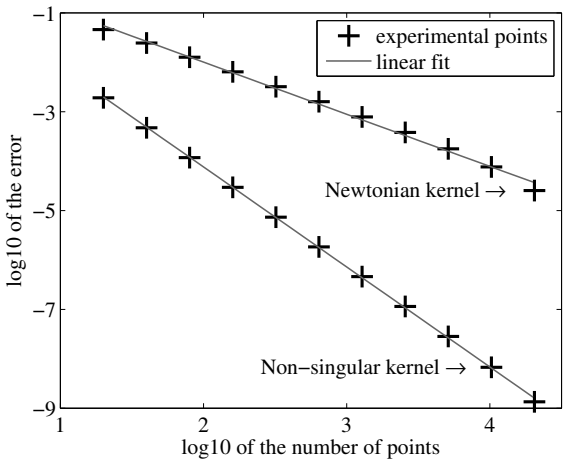

Figure 8: Logarithm of the error with respect to the number of points, with linear fit $y = px + q$, shown are the Newtonian potential and a smooth kernel $K(x) = e^{-\frac{x^2}{2}}$.

Acknowledgments

We thank Betsy Stovall for helpful comments regarding Lemma 2.7. This research is supported by NSF grants DMS-0907931 and DMS-1109805.

Bibliography

1. Luigi Ambrosio, Edoardo Mainini, and Sylvia Serfaty. Gradient flow of the chapman-rubinstein-schatzman model for signed vortices. *Annales de l'Institut Henri Poincaré (C) Non Linear Analysis*, 28(2):217 – 246, 2011.
2. Luigi Ambrosio and Sylvia Serfaty. A gradient flow approach to an evolution problem arising in superconductivity. *Comm. Pure Appl. Math.*, 61(11):1495–1539, 2008.
3. J. T. Beale, T. Kato, and A. Majda. Remarks on the breakdown of smooth solutions for the 3-D Euler equations. *Comm. Math. Phys.*, 94(1):61–66, 1984.
4. J. Bedrossian, Nancy Rodriguez, and Andrea L. Bertozzi. Local and global well-posedness for aggregation equations and Patlak-Keller-Segel models with degenerate diffusion. *Nonlinearity*, 24:1683–1714, 2011.
5. D. Benedetto, E. Caglioti, and M. Pulvirenti. A kinetic equation for granular media. *RAIRO Modél. Math. Anal. Numér.*, 31(5):615–641, 1997.
6. A. L. Bertozzi and P. Constantin. Global regularity for vortex patches. *Comm. Math. Phys.*, 152(1):19–28, 1993.
7. A.L. Bertozzi and T. Laurent. Finite-time blow-up of solutions of an aggregation equation in R^n. *Comm. Math. Phys.*, 274:717–735, 2007.
8. Andrea L. Bertozzi. Heteroclinic orbits and chaotic dynamics in planar fluid flows. *SIAM J. Math. Anal.*, 19(6):1271–1294, 1988.
9. Andrea L. Bertozzi and Jeremy Brandman. Finite-time blow-up of L^∞-weak solutions of an aggregation equation. *Commun. Math. Sci.*, 8(1):45–65, 2010.
10. Andrea L. Bertozzi, José A. Carrillo, and Thomas Laurent. Blow-up in multidimen-

sional aggregation equations with mildly singular interaction kernels. *Nonlinearity*, 22(3):683–710, 2009.
11. Andrea L. Bertozzi, John B. Garnett, and Thomas Laurent. Characterization of radially symmetric finite time blowup in multidimensional aggregation equations, 2011.
12. Andrea L. Bertozzi, Thomas Laurent, and Jesús Rosado. L^p theory for the multidimensional aggregation equation. *Comm. Pure Appl. Math.*, 64(1):45–83, 2011.
13. Andrea L. Bertozzi and Dejan Slepčev. Existence and uniqueness of solutions to an aggregation equation with degenerate diffusion. *Commun. Pure Appl. Anal.*, 9(6):1617–1637, 2010.
14. Piotr Biler and Wojbor A. Woyczyński. Global and exploding solutions for nonlocal quadratic evolution problems. *SIAM J. Appl. Math.*, 59(3):845–869 (electronic), 1999.
15. Adrien Blanchet, José A. Carrillo, and Nader Masmoudi. Infinite time aggregation for the critical Patlak-Keller-Segel model in $\mathbb{R}^2$. *Comm. Pure Appl. Math.*, 61(10):1449–1481, 2008.
16. Adrien Blanchet, Jean Dolbeault, and Benoît Perthame. Two-dimensional Keller-Segel model: optimal critical mass and qualitative properties of the solutions. *Electron. J. Differential Equations*, pages No. 44, 32 pp. (electronic), 2006.
17. M. Bodnar and J. J. L. Velazquez. An integro-differential equation arising as a limit of individual cell-based models. *J. Differential Equations*, 222(2):341–380, 2006.
18. Silvia Boi, Vincenzo Capasso, and Daniela Morale. Modeling the aggregative behavior of ants of the species *polyergus rufescens*. *Nonlinear Anal. Real World Appl.*, 1(1):163–176, 2000. Spatial heterogeneity in ecological models (Alcalá de Henares, 1998).
19. Michael P. Brenner, Peter Constantin, Leo P. Kadanoff, Alain Schenkel, and Shankar C. Venkataramani. Diffusion, attraction and collapse. *Nonlinearity*, 12(4):1071–1098, 1999.
20. Martin Burger, Vincenzo Capasso, and Daniela Morale. On an aggregation model with long and short range interactions. *Nonlinear Anal. Real World Appl.*, 8(3):939–958, 2007.
21. Martin Burger and Marco Di Francesco. Large time behavior of nonlocal aggregation models with nonlinear diffusion. *Netw. Heterog. Media*, 3(4):749–785, 2008.
22. Thomas F. Buttke. A fast adaptive vortex method for patches of constant vorticity in two dimensions. *J. Comput. Phys.*, 89(1):161–186, 1990.
23. Luis Caffarelli and Juan Vázquez. Nonlinear porous medium flow with fractional potential pressure. *Archive for Rational Mechanics and Analysis*, pages 1–29, 2011. 10.1007/s00205-011-0420-4.
24. J. A. Carrillo, M. DiFrancesco, A. Figalli, T. Laurent, and D. Slepčev. Global-in-time weak measure solutions and finite-time aggregation for nonlocal interaction equations. *Duke Math. J.*, 156(2):229–271, 2011.
25. José A. Carrillo, Robert J. McCann, and Cédric Villani. Kinetic equilibration rates for granular media and related equations: entropy dissipation and mass transportation estimates. *Rev. Mat. Iberoamericana*, 19(3):971–1018, 2003.
26. José A. Carrillo, Robert J. McCann, and Cédric Villani. Contractions in the 2-Wasserstein length space and thermalization of granular media. *Arch. Ration. Mech. Anal.*, 179(2):217–263, 2006.
27. José A. Carrillo and Jesús Rosado. Uniqueness of bounded solutions to aggregation equations by optimal transport methods. In *European Congress of Mathematics*, pages 3–16. Eur. Math. Soc., Zürich, 2010.
28. Jean-Yves Chemin. Persistance de structures géométriques dans les fluides incompressibles bidimensionnels. *Ann. Sci. École Norm. Sup. (4)*, 26(4):517–542, 1993.
29. Jean Dolbeault and Benoît Perthame. Optimal critical mass in the two-dimensional

Keller-Segel model in $\mathbb{R}^2$. *C. R. Math. Acad. Sci. Paris*, 339(9):611–616, 2004.
30. Hongjie Dong. On similarity solutions to the multidimensional aggregation equation, 2011. http://arxiv.org/abs/1102.0177.
31. David G. Dritschel. A fast contour dynamics method for many-vortex calculations in two-dimensional flows. *Phys. Fluids A*, 5(1):173–186, 1993.
32. David G. Dritschel and Norman J. Zabusky. A new, but flawed, numerical method for vortex patch evolution in two dimensions. *J. Comput. Phys.*, 93(2):481–484, 1991.
33. Qiang Du and Ping Zhang. Existence of weak solutions to some vortex density models. *SIAM J. Math. Anal.*, 34(6):1279–1299 (electronic), 2003.
34. Weinan E. Dynamics of vortex liquids in Ginzburg-Landau theories with applications to superconductivity. *Physical Review B*, 50(2):1126–1135, 1994.
35. Veysel Gazi and Kevin M. Passino. Stability analysis of swarms. *IEEE Trans. Automat. Control*, 48(4):692–697, 2003.
36. Darryl D. Holm and Vakhtang Putkaradze. Formation of clumps and patches in self-aggregation of finite-size particles. *Phys. D*, 220(2):183–196, 2006.
37. Yanghong Huang and Andrea L. Bertozzi. Self-similar blowup solutions to an aggregation equation in $\mathbf{R}^n$. *SIAM J. Appl. Math.*, 70(7):2582–2603, 2010.
38. E. F. Keller and L. A. Segel. Initiation of slime mold aggregation viewed as an instability. *J. Theor. Biol.*, 26:399415, 1970.
39. S. Kida. Motion of an elliptic vortex in a uniform shear flow. *J. Phys. Soc. Japan*, 50:3517–3520, 1981.
40. Gustav Kirchoff. *Vorlesungen über mechanik*. B. G. Teubner, Leipzig, 1897.
41. Sir Horace Lamb. *Hydrodynamics*. Cambridge University Press, 1932. sixth edition.
42. Thomas Laurent. Local and global existence for an aggregation equation. *Comm. Partial Differential Equations*, 32(10-12):1941–1964, 2007.
43. Dong Li and Jose Rodrigo. Finite-time singularities of an aggregation equation in $\mathbb{R}^n$ with fractional dissipation. *Comm. Math. Phys.*, 287(2):687–703, 2009.
44. Dong Li and Jose L. Rodrigo. Refined blowup criteria and nonsymmetric blowup of an aggregation equation. *Adv. Math.*, 220(6):1717–1738, 2009.
45. Dong Li and Xiaoyi Zhang. On a nonlocal aggregation model with nonlinear diffusion. *Discrete Contin. Dyn. Syst.*, 27(1):301–323, 2010.
46. Hailiang Li and Giuseppe Toscani. Long-time asymptotics of kinetic models of granular flows. *Arch. Ration. Mech. Anal.*, 172(3):407–428, 2004.
47. Fanghua Lin and Ping Zhang. On the hydrodynamic limit of Ginzburg-Landau vortices. *Discrete Contin. Dynam. Systems*, 6(1):121–142, 2000.
48. Edoardo Mainini. A global uniqueness result for an evolution problem arising in superconductivity. *Boll. Unione Mat. Ital. (9)*, 2009.
49. Edoardo Mainini. Well-posedness for a mean field model of Ginzburg-Landau vortices with opposite degrees, 2010.
50. Andrew J. Majda and Andrea L. Bertozzi. *Vorticity and incompressible flow*, volume 27 of *Cambridge Texts in Applied Mathematics*. Cambridge University Press, Cambridge, 2002.
51. Nader Masmoudi and Ping Zhang. Global solutions to vortex density equations arising from sup-conductivity. *Ann. Inst. H. Poincaré Anal. Non Linéaire*, 22(4):441–458, 2005.
52. A. Mogilner, L. Edelstein-Keshet, L. Bent, and A. Spiros. Mutual interactions, potentials, and individual distance in a social aggregation. *J. Math. Biol.*, 47(4):353–389, 2003.
53. Alexander Mogilner and Leah Edelstein-Keshet. A non-local model for a swarm. *J. Math. Biol.*, 38(6):534–570, 1999.

54. Daniela Morale, Vincenzo Capasso, and Karl Oelschläger. An interacting particle system modelling aggregation behavior: from individuals to populations. *J. Math. Biol.*, 50(1):49–66, 2005.
55. J.C. Neu. The dynamics of a columnar vortex in an imposed strain. *Physics of Fluids*, 27:2397–2402, 1984.
56. Juan Nieto, Frédéric Poupaud, and Juan Soler. High-field limit for the Vlasov-Poisson-Fokker-Planck system. *Arch. Ration. Mech. Anal.*, 158(1):29–59, 2001.
57. Frédéric Poupaud. Diagonal defect measures, adhesion dynamics and Euler equation. *Methods Appl. Anal.*, 9(4):533–561, 2002.
58. R. Robert. Unicité de la solution faible à support compact de léquation de Vlasov Poisson. *C. R. Acad. Sci. Sér. I*, 324:873877, 1997.
59. Étienne Sandier and Sylvia Serfaty. A rigorous derivation of a free-boundary problem arising in superconductivity. *Ann. Sci. École Norm. Sup. (4)*, 33(4):561–592, 2000.
60. Etienne Sandier and Sylvia Serfaty. *Vortices in the magnetic Ginzburg-Landau model*. Progress in Nonlinear Differential Equations and their Applications, 70. Birkhäuser Boston Inc., Boston, MA, 2007.
61. E. M. Stein. *Harmonic Analysis: Real-Variable Methods, Orthogolaity, and Oscillatory Integrals*. Princeton University Press, 1993.
62. Chad M. Topaz and Andrea L. Bertozzi. Swarming patterns in a two-dimensional kinematic model for biological groups. *SIAM J. Appl. Math.*, 65(1):152–174 (electronic), 2004.
63. Chad M. Topaz, Andrea L. Bertozzi, and Mark A. Lewis. A nonlocal continuum model for biological aggregation. *Bull. Math. Biol.*, 68(7):1601–1623, 2006.
64. Giuseppe Toscani. One-dimensional kinetic models of granular flows. *M2AN Math. Model. Numer. Anal.*, 34(6):1277–1291, 2000.
65. V. I. Yudovich. Non-stationary flow of an ideal incompressible liquid. *USSR Computational Mathematics and Mathematical Physics*, 3(6):1407 – 1456, 1963.
66. Norman J. Zabusky, M. H. Hughes, and K. V. Roberts. Contour dynamics for the Euler equations in two dimensions. *Journal of Computational Physics*, 30(1):96–106, 1979. reprinted in JCP vol. 135, pp. 220-226, 1997, 30 year anniversary issue.